ISSN No:-2456-2165

Preyssler Polyoxometalate an Overview

Olivia Neogi
School of Chemistry-University of Hyderabad

Abstract:- Preyssler Polyoxometalate (POM) is a doughnut shaped heteropolytungstate constructed from five PW6O22 units, each of which is derived from the lacunary fragment of Keggin anion, α-[PW12O40]3-. They are the first examples of POMs with an internal cavity within which remains encrypted a sodium cation. This sodium cation can be replaced for trivalent lanthanide cations and other cations of similar size. Hence, Preyssler POM is also called inorganic crown ethers or inorganic cryptrates. Preyssler POM is a redox active cluster which is active over a wide range of pH from 0 to 10. As said, the encrypted lanthanide is usually in +III oxidation state. However, Europium and Cerium encrypted POMs shows certain behaviour that lead the chemists to predict +II and +IV Oxidation states respectively . However, XANES, EXAFS, CV confirmed an oxidation state of +III in the above cases. Cyclic voltammetry reveals an extensive redox chemistry of the lanthanide encrypted POMs. Dyprosium and Holmiun encrypted POMs are found to exhibit single molecular magnetism. The study on the surface of Preyssler POM is highly explored and has ruled almost a decade. Various reseachers employed various techniques like layer-by-layer mechanism and Ionic self-Assembly process for the construction of multilayer composites and nanostructures and subjected them to the study of electrochromism. Preyssler POM has been for lesser number of times employed as a building block for the construction of extended strutures, owing to the discrepancy in obtaining single crystal. A handful of examples have been elucidated below. The example of the lacunary Preyssler POM and an extended structure based on it have also been set up. Preyssler POM has been observed to make its most remarkable contribution in the field of catalysis. Preyssler POM is found to be a green catalyst and has efficiently catalysed a huge number of organic reactions. The medicinal value of Preyssler POM has also been established. A number of theoretical studies have also been performed.

Keywords:- *Preyssler, Polyoxometalates, Cryptohydration, Hysterysis, Electrochromism*

I. INTRODUCTION

The progress in the field of Solid State Inorganic chemistry is being strongly driven by its substantial relevance to the world trade. In keeping with the custom, inorganic chemists have been meticulously probing on molecules that are versatile in terms of its properties and which exhibit unique potential applications. A very preferred class of compounds which has fascinated the inorganic chemists round the globe and which seems to exhibit remarkable properties, morphologies and applications are Polyoxometalates (POMs). Besides, they have been an academician's fascination too inasmuch their well –defined shape, size and the architectural beauty are taken into account. Polyoxometalates are anionic nano clusters made up of several oxygen atoms and early transition metals like W, V, Mo, Nb etc. that exhibit an unsurpassed range of physical properties and unique potential applications in catalysis, magnetism, solar energy conversion, biology etc. The increasing contemporary curiosity of chemists about polyoxometalates started in early 1990's when two pioneering scientists, Pope and Muller of this field noted their exciting features and published a broad review article on it.[1] Thereafter, a number of thematic review articles were published by various notable researchers of the field. Inspite of the passage of a century since the birth of this field that the inorganic chemists are still concentrating on POMs is perhaps because of the high combinatorial possibilities leading to very many structures each of which again lead to material of promising applicability. [2] Few basic example of POMs include Keggin POM {[XM12O40] n−}, Well Dawson ([X2M18O62}q-), Anderson POM [MMo6H5O24]x- etc. Of our particular interest, is a large polytungstate anionic cluster, called Preyssler POM, based on the lacunary fragments of Keggin POM endowed with striking architectural significance and electroactivity.

II. BACKGROUND

A. History

The story of Preyssler POM began when, C. Preyssler as early as in 1970, while preparing ammonium octadecatungstodiphosphate, $(NH_4)_6P_2W_{18}O_6$, observed white crystals long before the formation of the desired product. He formulated them as $(WO_3)_{18}(PO_4)_3H(NH_4)$ on the basis of chemical analyses like potentiometric, titration, and cryoscopic measurements. Thereafter, ^{31}P NMR measurements were carried out elsewhere to reveal, that all the phosphorus atoms of this polytungstate were equivalent and the ^{183}W NMR spectrum (recorded independently by another group) consisting of four lines (intensities 2:2:1:1) indicated a different stoichiometry than that proposed by Preyssler.

B. Synthetic Strategy of Preyssler POM

- *Conventional Reflux:*

The synthetic stategy as employed by C. Preyssler himself with a slight change thereof was given as follows:

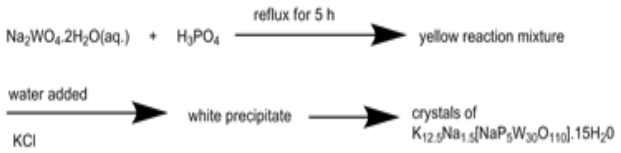

To an aqueous solution of sodium tungstate dihydrate, was added phosphoric acid. The resulting mixture was refluxed for five hours at 80ºC to obtain a yellow reaction mixture. The yellow reaction mixture was cooled to room temperature and an aqueous solution of potassium chloride was added to it. The white solid as separated was dissolved in warm water to obtain the crystals of sodium potassium salt of Preyssler POM with fifteen water molecules of crystallization.

➢ *Hydrothermal Synthesis:*

With an aim of obtaining a more appropriate crystal, Pope along with Jeannin and others reinvestigated the story and adopted a different synthetic stategy altogether. They synthesized the Preyssler POM by the hydrothermal method which happenned to be as follows:

The mixture of an aqueous solution of sodium tungstate dihydrate and phosphoric acid were enclosed in a bomb and was heated overnight at 120ºC.After taking out, the bomb was cooled to room temeprature and water was added to the yellow reaction mixture followed by the addition of potassium chloride. The white precipitate as obtained was dissolved in hot water to obtain the crystals of sodium potassium salt of Preyssler anion. The product was also obtained in a better yield.

➢ *Different Counterions:*

A group changed the counteraction for different other counterions like Cs, Ba, La, Ce, Hg, Tl,Pb and Bi and studied their effect on the anion.[3] Due to the difference in the charge and size, different amounts of cations appeared in the Hetropolyanion and rest of the charges were compensated with proton. While the free acid and Cs derivative was found to be soluble in water, Ba, La and Ce substituted POMs were found to be slightly soluble and rests were insoluble in water. La, Ce and Pb derivatives formed a turbid solution in water at 55ºC and formed clear oil at 60ºC.These floated in water and formed a pseudoliquid phase. In fact the compound adsorbed a large amount of water in their networks and turned into liquid phase rather than getting dissolved in water.

TGA showed an endothermic peak in the DSC curve due to the physically adsorbed water. Ba derivative showed two endothermic peaks below 100ºC indicating two staged water release. The endothermic peaks around 150-420ºC were due to the loss of water of crystallization. At higher temperature, decomposition of the heteropolyanion occurred with the appearance of exothermic peaks and an increase in the weight attributable to the formation of oxides. Ce-derivative showed the highest thermal stability and the Hg derivative showed the least thermal stability. The types of the counterions prominently affected the chemical behavior, redox properties and the catalysis.

BET measurements showed that the surface area of only Cs, Ba and Tl derivatives could be measured at a temperature below 125ºC and rest showed negative slopes in the BET plots. Ba derivatve with high surface area and porous structure showed a negative slope. This was perhaps because of the delocalization of the received electrons produced from the heating of the heteropolyacids.

CV of the Preyssler HPA with the various contercations showed similar electrochemical behavior which indicated that they were structurally similar. The positions of the catholic and anodic waves were found to be in agreement with the previously reported values. However, the anodic waves of Bi, Hg and Pb were found to be complicated due to the reduction of the ions in cathodic cycles which raised the conductivity of the return cycle. The oxidation of the heteropolyacid was found to be more sensitive to counter ions than the reduction. Thus, H^+ derivative readily lost electrons whereas Ce derivative showed the least tendency to oxidize.

The IR spectra showed similarity in the values excepting the W=O stretching frequencies indicating the retaining of the heteropolyacid structure. A large shift observed in cases of H^+ and Cs^+ could be due to their interaction with the oxo groups. On the other hand, the P-O vibrations were not affected by the W=O stretching frequencies due to their core bonding nature. The water molecule bending vibration also showed no dependency on the counteraction type.

XPS studies revealed similar binding energies of oxygen 1p and phosphorous 2p in all compounds which indicated at the independency of the heteropolyanion core on the cation. The binding energies of the surface-located oxygens and and tungsten were identical for the whole series which indicated that the cations and anions were discrete species. The binding energy of W 4f for the Tl salt was different from others and showed an accumulation of more positive charge on the tungsten atom. The occurrence of three peaks instead of two for H^+ and Cs^+ further confirmed the interaction of the counterions with the oxo groups.

III. STRUCTURE

➢ *Original Structure:*

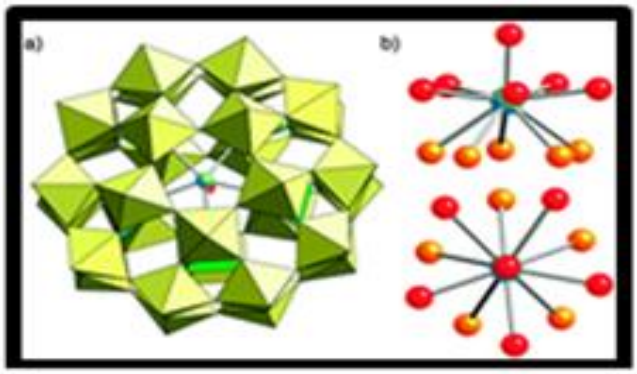

Fig 1 Structure of Preyssler POM, C_5 passing through the central cation.

The hydrothermal synthesis of Preyssler POM furnished better crystals which allowed Pope and his co-workers to successfully solve the structure. Thus, the structure of Preyssler POM was for the first time revealed in 1985, fifteen years ever since after its discovery. This is the reason why Preyssler POM is also termed as Preyssler-Jeannin-Pope (PJP) POM. It were they who formulated the Preyssler heteropolyanion as $[NaP_5W_{30}O_{110}]^{14-}$ and said that it was a doughnut shaped heteropolytungstate , electroactive and stable at a wide pH range of 0-10. The rotationally symmetrical ellipsoid (or the oblate spheroid with D_{5h} point group as mentioned) was found to be constructed from five PW_6O_{22} units, each of which was derived from the lacunary fragment of Keggin anion, α-$[PW_{12}O_{40}]^{3-}$. The five units were wedged to one another by corner-sharing of WO_6 polyhedron giving rise to an oblate spheroid.

➢ *Structural Change :*

Kortz and his co-workers showed that $[Na_5W_{30}O_{110}]^{14-}$ was close to its structural change of fourteen elementary negative charges in the presence of linear polyamines.[82] Polyelectrolytes complexes were obtained by mixing oppositely charged polyelectrolytes. The Kortz group investigated the ion-pair formation between Preyssler POM and two different polycations, poly(L-lysine hydrobromide) (PLL) and poly(allylamine hydrobromide) (PAH) for zeta potential and conductometry.The work was carried out in solution of low ionic strength in order to decrease the screening of electrostatic interactions between POM and polyelectrolyte. The pH of the solution varied with the increase in the ratio of number of moles of P_5W_{30} to that of monomer and conductivity of solution increased. Such pH could result in the full protonation polycation. The turbidity increased too with the increase in the molar ratio of POM and Polycations. The maximum in the turbidity corresponded to the formation of aggregates which occurred due to the neutralization of the charged pair.

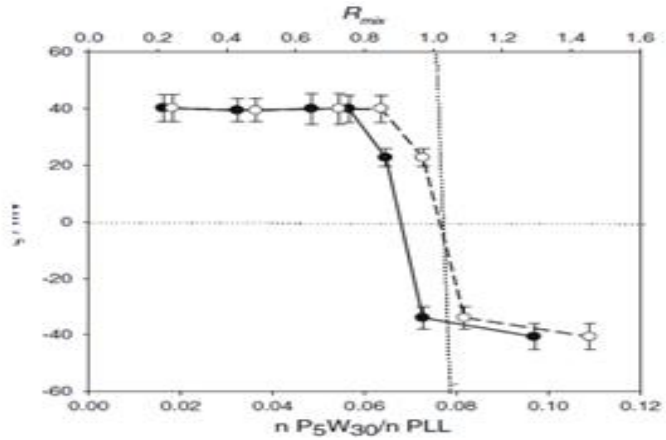

Fig 2 Zeta-potential of P_5W_{30} ion pair

As the pH of the solution increased during the titration of PLL by P_5W_{30}, some H_3O^+ were replaced by OH^- ions which brought a change in the conductivity of the solution. Hence, the plateau in the above Fig. 51. The counterion release from PLL(Br^-) and $P_5W_{30}(Na^+)$ was calculated according to the following equation:

$$\Delta\kappa_{total} = \Delta\kappa_{pH\ change} + \Delta\kappa_{NaBr}$$

The conductivity was calculated to be increased and it was due to the increase in the NaBr concentration. From all the calculations, it could be concluded that that each P5W30 unit released 14 Na^+ counterions and the uncertainty in this amount of the released Na+ per polyanion was about ±1. Thus, the polyanion behaved as a colloid carry fourteen elementary charges. The maxima of the turbidity occurred at mixing ratio(R_{mix}) of 1. The zeta potential changed from positive and almost constant values to negative and constant negative zeta potential values. The ion pair prepared in the presence of a large excess of polycations had the same value o zeta potential forming them.

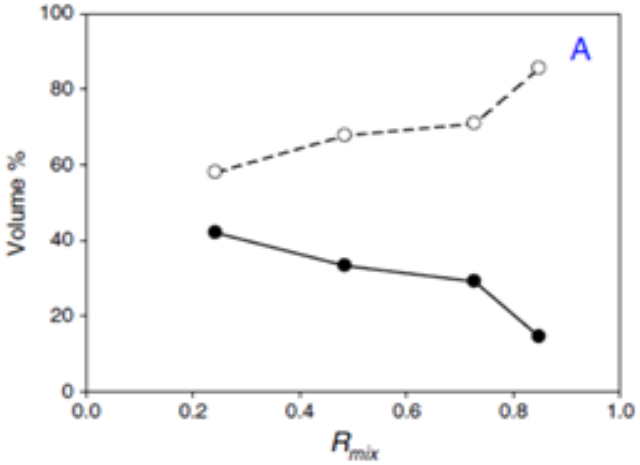

Fig 3 Volume percent of large and small ion pair as a function of mixing ratio.

➢ *Crystallographic Studies:*

Crystallographic studies showed a triclinic unit cell for the anion with a space group of *Pi* and the data collected thereof revealed a minor axis of 12.71 A^o and major axes with minimum face-to face dimension of 16.70 A and corner-to-corner dimension of 17.39 A^o. [4] The anion was the first example of a polyoxometalate with an internal cavity having sodium ion encapsulated within. X-Ray studies revealed that the Na^+ did not exactly sit into the cylindrical cavity but was slightly displaced along the vertical C_5 axis. This removed the σ_h symmetry plane and reduced the symmetry to C_{5V}.[5] The tungsten atoms were distributed in four planes perpendicular to the principal C_5 axis. The outer planes consisted of five tungsten atoms each and the inner planes consisted of ten tungsten atoms each.

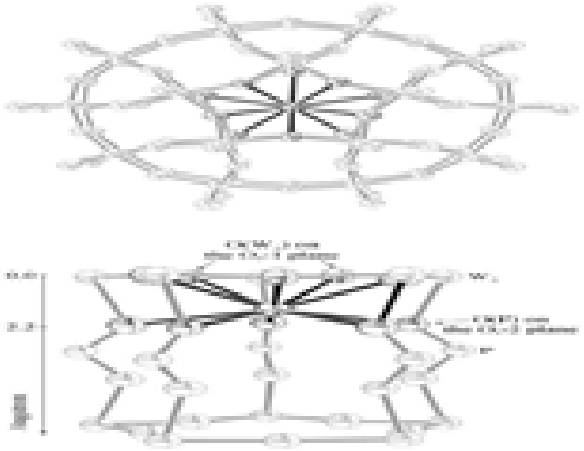

Fig 4 Top view of Preyssler anion $[M^{n+}P_5W_{30}O_{110}]^{(15-n)+}$

Removal of W_3O_{13} unit from the Keggin structure resulted in PW_9 unit of P_2W_{18} unit of Dawson anion. Further removal of W_3 resulted in PW_6 unit and the entire molecule could be viewed as an assembly of PW_6 units on the Na^+ metal center built up in template fashion. Each PW_6 unit was bound to two other such units using eight oxygen atoms resulting in corner shared octahedral. There were several vacant sites inside the polyanion, along the principal fivefold axis. The first cavity, site S1 was located at the mirror plane surrounded by ten oxygen atoms, thus making the two parallel planes of tungsten related by the mirror planes. Two other equivalent sites were located at the C_5 axis, related to each other via a mirror plane. S2 was defined by five oxygens from one of the previously mentioned pentagons and five other oxygens from another pentagon of outer parallel plane. Na^+ occupied a site near site S2 slightly displaced towards the center of the anion. Preyssler POM was thus the inorganic analogue of crown ether and other organic cryptands. There was also a water molecule linked with the central sodium ion. After assembly, the central Na^+ ion, under severe experimental conditions could be exchanged for other ions of similar size.

➢ *P-XRD Pattern :*

The powder XRD pattern of Preyssler POM is as follows:

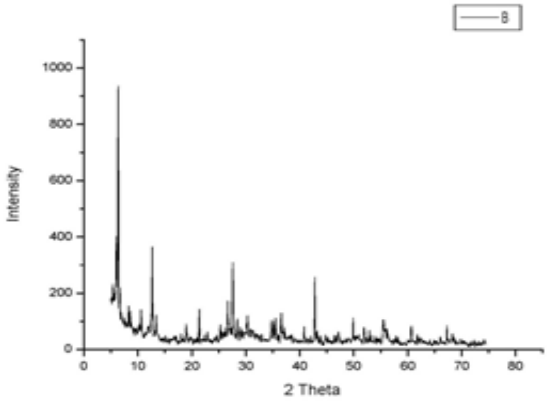

Fig 5 Powder XRD pattern of Preyssler POM

➢ *Scanning Tunneling Microscope:*

In 1997, Kaba *et. al.* imaged the molecular shape, orientation and packing of atoms in Preyssler anion through Scanning Tunnel microscopy.[7] In the ammonium salt of Preyssler anion, the atoms were found to be arranged in an oblique fashion between them with a periodicity of 13.8±0.2 A^0×19.5±0.2 A^0. The lattice spacing along the minor axis was in good agreement with the (010) of the bulk structure. The ammonium counteraction, (relative to potassium cation) to the Preyssler anion increased the lattice constant of the two-dimensional Preyssler POM by 0.5 A^0 along the minor axis and 1 A^o along the major axis.

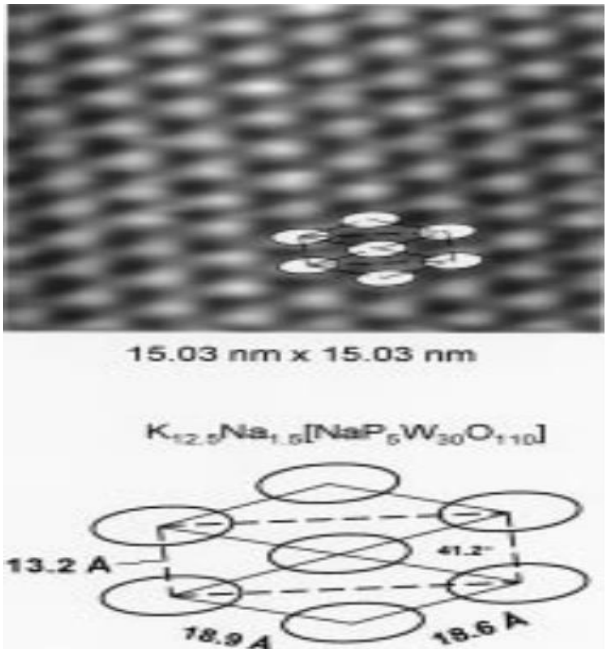

Fig 6 STM image of $K_{12.5}Na_{1.5}[NaP_5W_{30}O_{110}]$

The STM imaging clearly revealed that while the potassium salt of PJP anion was a centered rectangular lattice, the ammonium salt of the same was evidently oblique. Again, while the five-fold axes of the anions in the surface arrays of potassium salt were found to be collinear, that in ammonium salt was found be not. Thus, the identity

of counter-cation not only influenced the lattice spacing but also the lattice symmetry of the two-dimensional arrays of Preyssler POM. However, the fine-tuning of the anionic structure was not possible because of (1) the separation of the molecular anions by water molecules of hydration and (2) the reduction of the overall symmetry from D_{5h} to C_5v further created disorder thereby decreasing the scattering power of X-rays.

However, for an exact understanding of the bonding involved therein and the properties exhibited thereby, the above drawbacks were supposed to be got ridded of. A detailed EXFAS study by Soderholm *et. al.* in the year 2004, served as a way out of the above problems. The X-ray Absorption Spectroscopy (XAS) provided methodical information about the position of the cation within the Preyssler cavity. The data collected thereof did not change upon the exchange of the encapsulated cation for another. The data as modeled by bond valence approach helped to provide a deep understanding of the stabilities of the metal ion in different oxidation states and their redox activities.

➢ *Exafs:*

The peaks obtained from the plot of $k^3\chi(k)$ versus k M^{n+} for various metal encapsulated Preyssler anion ($M=Sr^{2+}$, Y^{3+}, Th^{4+}) reasonably explained the metal encrypted Preyssler anion . The EXFAS studies clearly indicated that the interatomic distance within the Preyssler anion varied as function of the charge to the ionic radius ratio of the encrypted cation. For e.g. while going from highest cationic radii(U^{4+}) to lowest ionic radii (Sr^{2+}) , the M-W distance of the anion gradually showed an increase from 3.54 A^O to 3.56A^O and M-P distance showed a decrease from 4.03 A^o to 3.65 A^o thereby exhibiting the greatest deviation. The above drift clearly indicated that the cation was displaced along the vertical C_5 axis of the anion thereby agreeing with the previously derived conclusion. However, only a limited number of metals could be encrypted within the cavity due to the non-ideal coordination environment available as also because of the accessibility of the sole degree of freedom along the C_5 axis.

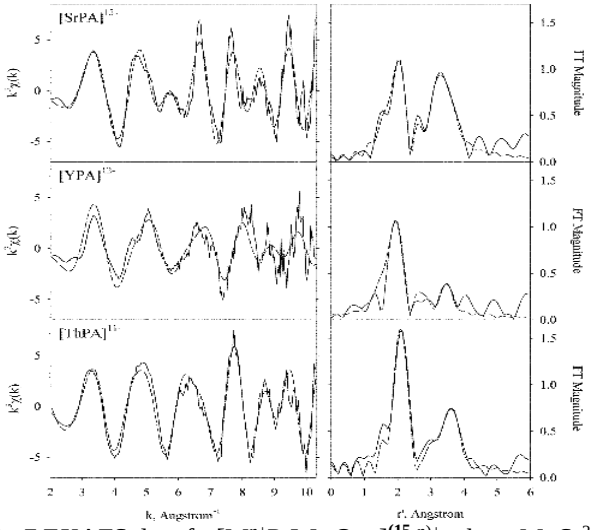

Fig 7 EXAFS data for$[M^{n+}P_5W_{30}O_{110}]^{(15-n)+}$ where $M=Sr^{2+}$, Y^{3+}, Th^{4+}

➢ *Cryptohydration:*

The crystal structure of Preyssler anion showed site disorder of counterions or both, the disorder being attributed to their high symmetry allowing them to assume two or more orientations at one crystallographic site.[8] Thus, the cations or water exhibited fractional occupancy among several sites. Preyssler anion had two possible coordination sites. One S1at the centre, formed by the plane of ten phosphate oxygen atoms and the other S2 formed by five phosphate oxygens and five W-O-W oxygen atoms and there existed two equivalent S2 sites per anion. Eg. In Na-POM, the Na^+ cation was equally disorded between the two S2 sites. Thus, for different encapsulated anions, the degree of occupancy varied.

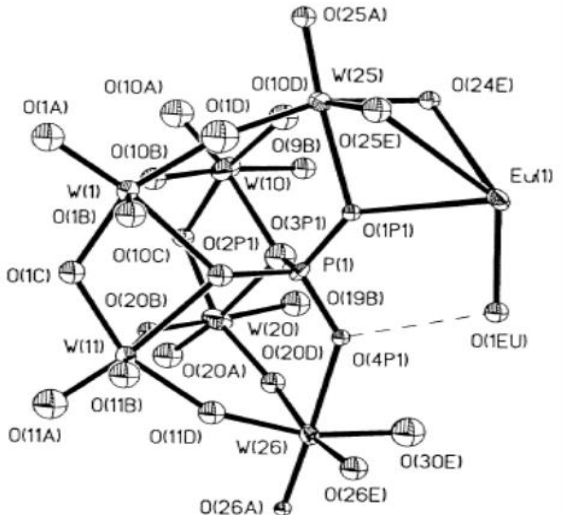

Fig 8 Position Of Atoms Within Preyssler POM

IV. SPECTROSCOPY

➢ *IR Spectroscopy:*

The IR frequencies of all the structures were found to be similar except that of P-O stretching frequency (1073 cm^{-1} for NaP_5W_{30} and 1060 cm^{-1} for ZP_5W_{30}).

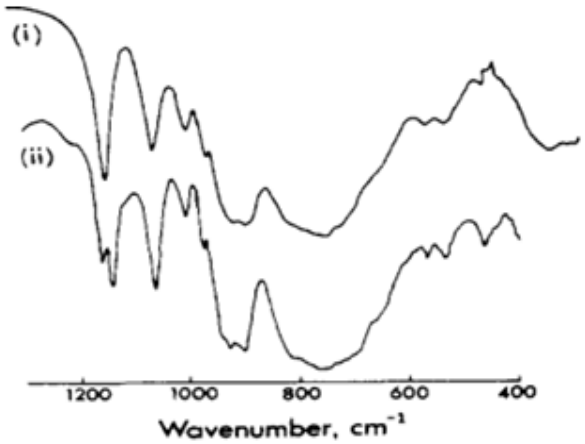

Fig 9 (i) IR of $[NaP_5W_{30}O_{110}]^{14-}$
(ii) IR when the solution of $[NaP_5W_{30}O_{110}]^{14-}$ is heated is Ca^{2+}

➢ *Optical Spectroscopy:*

- *UV-VIS Spectroscopy:*

Almost all the cation- containing Preyssler POMs showed a broad band in the range of 240-340 nm ε>17000 M-1Cm-1. Furthermore, there was one absorption band beyond 240 nm with large extinction co-efficient attributed to Charge Transfer. The lowest energy electronic transition occurred at 278 nm and there occurred a blue shift with the increase in the charge of the encapsulated cation (Th4+). The plot of potential vs. charge showed a linear least square fit.

- *^{23}Na NMR:*

^{23}Na NMR showed a broad line at slightly different frequency from the free sodium ion. 23Na NMR of YP5W30 was taken to find no signal of sodium. This indicated at the displacement of sodium and no attachment at any other site of the heteropolyanion.

- *^{31}P NMR:*

Table 1 The Data Are Tabulated As Under: [19]

Z^{n+}	δ/ppm	$\Delta\nu_{1/2}$/Hz
Nd^{3+}	-15.0	8.8
Sm^{3+}	-9.5	4.6
Eu^{3+}	0.7	5.0
Gd^{3+}	_	_
Tb^{3+}	27.2	175
Dy^{3+}	-68.1	241
Ho^{3+}	-40.0	222
Er^{3+}	1.8	151
Tm^{3+}	17.6	68
Yb^{3+}	9.1	16
Lu^{3+}	-10.1	_
Y^{3+}	-10.2 (d)	_
Bi^{3+}	-8.2	_
Ce^{4+}	-16.0	4.5
U^{4+}	-15.5	5.5
Na^{+}	-9.4	_
Ca^{2+}	-11.1	_

- *^{183}W NMR:*

^{183}W NMR in 1M DCl showed four signals with intensities in the ratio of 2:2:1:1 which corresponded to the two W-O planes containing 10 oxygen atoms and other two containing five oxygen atoms, each perpendicular to the C5 axis. The intensities when integrated gave downfield peaks for W-10 planes and upfield peaks for W-5 planes. This result was in consistency with the X-ray crystallography and EXAFS studies and indicated at the reduction of the overall symmetry of Preyssler POM from D5h to C5v owing to the displacement of the encapsulated cation along the principal axis. The distance between two downfield peaks increased with the increase in the charge of the encrypted cation as the position of the upfield peaks remained unchanged. The larger separation between the W-5 signals indicated a larger separation between the cation and the W-5 planes relative to the W-10 planes. In addition to the major 183W NMR peaks, two small coupling peaks of P-O-W and W-O-W (owing to the coupling between the corner-shared WO6 octahedral units) were also observed.

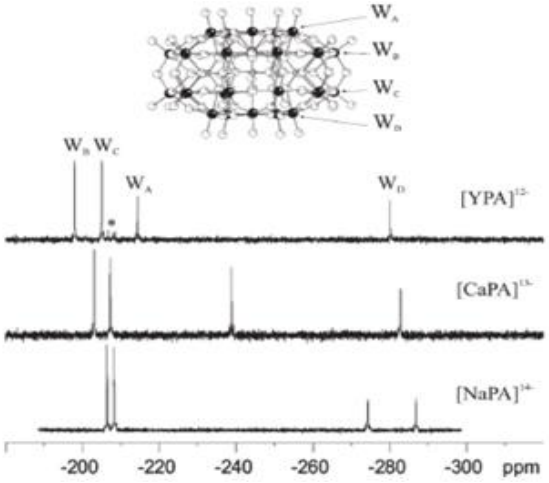

Fig 10 ^{183}W of different cation substituted Preyssler POM

V. ELECTROCHEMISTRY

The heteropolytunstate was reducible to heteropoly blue species. The first two reduction steps corresponded to four electrons each shown in Fig. 1 below. At pH 10, the first reduction step had split into a sequence of one electron reductions as seen in most of the heteropolytungstates. Sequential controlled potential electrolyses resulted in quantitative addition of one, two three and four electrons.

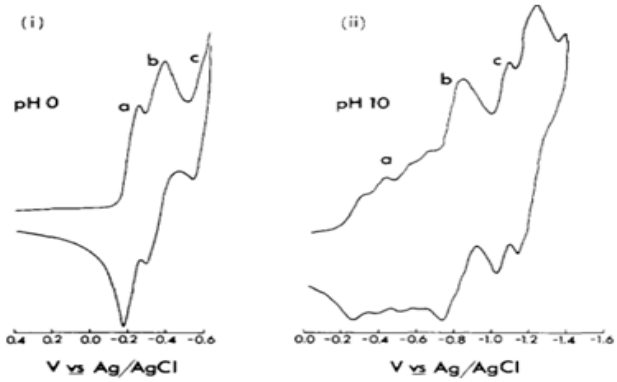

Fig 11 CV of Preyssler POM

The electronic absorption spectra showed a broad band at 14,300 cm^{-1}. The compound even though one electroned did not show paramagnetism perhaps because of the rapid intervalence electron transfer and /or extensive delocalization of through the corner-shared junctions of W_5 or W_{10} rings.

For $Y^{3+,}$ La^{3+} and Th^{4+} containing Preyssler POM, five reversible, two electron redox pairs were obtained. For Na^{+}, Ca^{2+}, Sr^{2+} exchanged Preyssler POM, three resolvable redox pairs were obtained, Out of which, two most positive ones showed shoulders, perhaps due to the overlapping pairs of redox couples. It was due to the decrease in the overall charge of the Preyssler anion that the reduction potential of the couple decreased. The plot of potential vs. charge showed a linear least square fit with a slope and intercept

which were in good agreement with the electrochemical studies of Keggin POM.

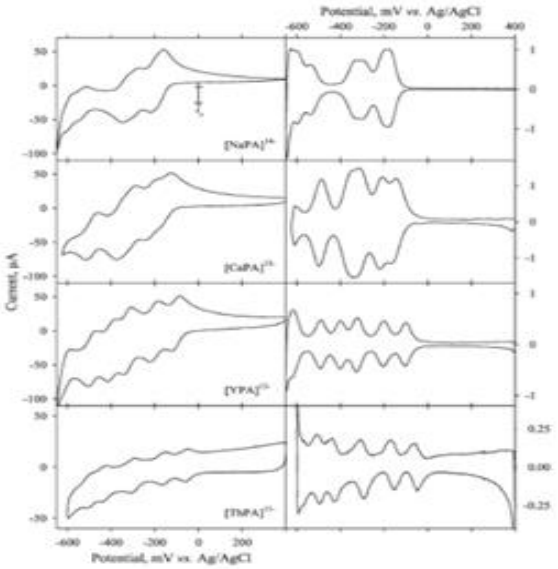

Fig 12 CV of $[NapA]^{14-}$, $CaPA]^{13-}$, $[YPA]^{13-}$, $ThPA]^{12-}$

Thus, the CV and optical spectroscopy data together with the reported calculations revealed that the 2P orbitals from W-O-W bridging oxygens formed the HOMO whereas the t_2g of d-orbitals of W formed LUMO. Distotion of high symmetry W resulted in the overall reduction of anti-bonding character of LUMO and the stabilization of d_{xy} orbitals with least Oxygen participation resulted in symmetry-adapted LUMOs.In keeping with the above electronic model, the UV bands were assigned to LMCT transitions from HOMO to LUMO.

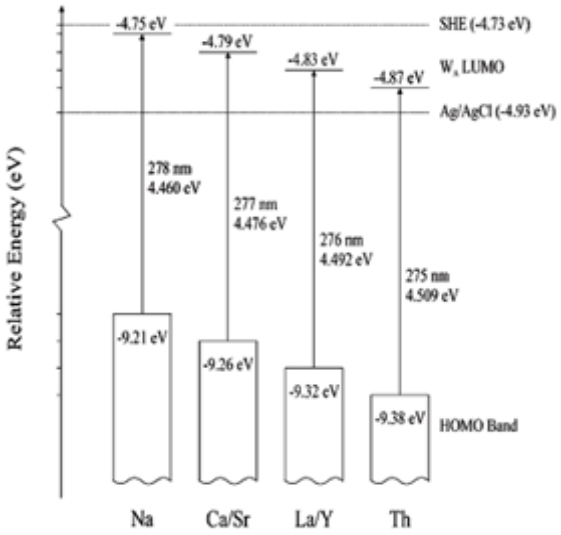

Fig 13 Frontier Molecular Energies And Its Change With The Increasing Charge Of The Cation

Thus, the combined study of electrochemistry and optical spectroscopy as supported by the NMR details provided an insight about the effect of the varying charge of the encrypted cation on the Preyssler framework.

VI. CHEMISTRY OF PREYSSLER POM

- *Ion exchange reaction and their charactization via EXAFS, XANES:*

So far, cations like Ca^{2+}, Bi^{3+}, Y^{3+}, trivalent lanthanides like La^{3+}, Ce^{3}+, Nd^{3+}, Eu^{3}+, tetravalent actinide like U^{4+} had been reported to replace the central sodium ion.[20] However, the cation was slightly displaced along the principal axis, the displacement being specific to the encyrpted cation (charge to radius ratio). The lanthanide-exchange as exhibited by the Preyssler anion had proven to be of immense importance in nuclear waste treatment. Antonio and Soderholm studied the energetics of the molecular orbitals of Preyssler POM by quantifying the effect of the charge of the cation on the electronic response of the Preyssler framework [21].

Table 2 Ion Exchange Reaction and their Charactization Via EXAFS, XANES

Z^{n+}	$T/^{O}C$	%yield
Pr	180	No reaction
Nd	180	<80
Sm	145-165	90
Eu	160	45-90
Gd	145	90
Tb	145	90
Dy	160	90
Ho	160	90
Er	160	90
Tm	160	90
Yb	160-180	50-70
Lu	180	40
Ce	160	50
Y	160	90
Bi	160	90
U	160	30
Ca	140	90
Z^{n+}	$T/^{O}C$	%yield
Pr	180	No reaction
Nd	180	<80
Sm	145-165	90
Eu	160	45-90
Gd	145	90
Tb	145	90
Dy	160	90
Ho	160	90
Er	160	90
Tm	160	90
Yb	160-180	50-70
Lu	180	40
Ce	160	50
Y	160	90
Bi	160	90
U	160	30
Ca	140	90

The cations, Na^{+}, Ca^{2+}, Sr^{2+}, Y^{3+}, La^{3+} and $Th^{4+,}$ were so chosen that they would only exhibit electrostatic bonding but not covalently bond with O^{2-} of POM. Also, owing to their diamagnetism and spherical symmetry, they would not

exhibit anisotropy or magnetic effects. The various temperatures at which the exchange reaction occurred are a given above.

Even though, the lanthanide ions got easily exchanged for Na^+ ion, exchange with other cations was not easy. The hard-soft concept also contributed to reactivity. The different cations containing Preyssler POM was stable at room temperature in 1M HCl. However, it decomposed to some other products at pH 9-10. Since, NaP_5W_{30} reacted with Lanthanide to different extent; it could be suitably employed for the separation of reaction mixture as was confirmed from the competition experiments. The more highly charged cations were located nearer the antiprism center formed from the five P-O oxygens and five bridging W-O-W oxygens so as to equalize the electrostatic interactions with the ten oxygen atoms.

However, the plot unlike as expected for an ideal electrochemical couple system was found to be nonlinear. Evidently, there are two linear regions in the graph with a crossover between them at a potential of -0.15V to -0.09V. At this potential range, the charge transfer occurs from the W-O framework of Preyssler anion to the lanthanide cation. This charge transfer was obtained by independently calculating the total counts of Coloumbs transferred to $[EuP_5W_{30}O_{110}]^{n-}$. Thus, the Nernst plot proved that the redox behaviour of Eu in $[EuP_5W_{30}O_{110}]^{n-}$ was irrelevant to that expected for a simple redox couple. This type of non-linear Nernst plot was seen in the case of Cytochrome C-oxidase due to the interaction of the two redox active centers Fe and Cu. The evidence of Non-linear Nernst plot was attributed to the very same reason of the interaction or hybridization (precisely) of the W-O centers and Eu f-states according to the equation:

$\Psi_{IV}=\alpha\varnothing_f + \beta\varnothing_f$
α = mixing co-efficient of f-state
β= mixing co-efficient of d-state

The hybridization occurred at a potential for which the unhybridized states would be almost degenerate. The constant r (E) was interpreted in terms of the addition of charge to the f-W-O band. XANES revealed that since the f-W-O band was partly composed of Eu-f states, electrons added to this band would have less influence on the observed final state valence. The two outer regions of the plot had slope different from n=1. This indicated that outside the highly correlated region, there existed weak interaction between the f_{Eu} and d_{W-O} states[22]. The f-d hybridization in Preyssler POM was attributed to the stereochemical factors which either favoured or hindered the orbital mixing of the ligand and the metal.Apart from the XANES study, magnetic studies of the solid that precipitated from solution at rest potential, final reducing potential, at -120 mV also individually supported the presence of f-d hybridization. The intermediate susceptibility values could also not be plotted linearly, and by being so, complied with the non-Nernstian plot. Thus Eu-POM gave a way to probe correlated electrons and non-integral valence.

- *Europium Exchanged Preyssler POM:*

The optical spectroscopy also evidenced in support of the presence of trivalent europium in $[EuP_5W_{30}O_{110}]^{n-}$.[23] The time –resolved fluorescence studies were executed using two different excitation laser energies. At an excitation energy of 19,030 cm^{-1}, Eu(III) was directly excited to $^5D_1$ multiplet. The first pathway of de-excitation observed was a direct fluorescence emission to $^7F_3$ associated with a weaker emission to $^7F_4$. The second pathway of emission was a non-radiative decay to $^5D_0$ which then fluoresced to ^7F_J multiplets. Owing to the difference in time delay, the two observed decay pathways could be separated experimentally.

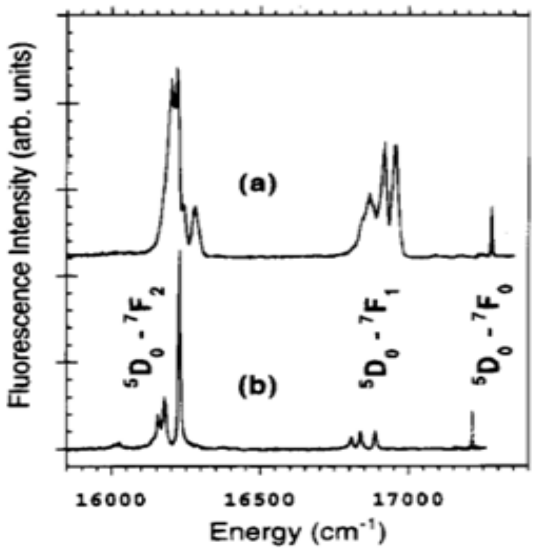

Fig 14 Fluorescence Spectra Obtained At An Excitation Of 19030 Cm-1 (B) At An Excitation Energy Of 18965 Cm-1.

Fluorescence spectroscopy indicated that all the Eu present were not equivalent and this prompted to take another optical experiment. Thus, in that experiment, the incident excitation energy was varied and the emitted polychromatic fluorescence was monitored. Those experiments confirmed the presence of a second structurally inequivalent Eu which showed different absorbtion and emission spectra. The two sites occupied by Eu was labelled as site A and site B . While Eu at site A could be observed at all measurable samples, Eu at site B could be seen only when more than 1 equivalent of Eu was present in the sample. The transition energies of the Eu atoms at the two different sites inevitably varied. The energy difference of 5D0 and 5D0 states of the two sites allowed one to perform the site selective excitations for their individual investigation. Considering the transition probabilities to be similar in both the cases, the ratio of Eu at site A was found to be 0.6 and at site B was found to be 0.4. The 7FJ multiplets were resolved for J=0, 1, 2, 3.The energies of the multiplets were found to be similar to that free Europium ion. Eu was found in low symmetry environments at both the sites. The dynamics of the two Eu sites were also looked for, for knowing the relative ratio of the Eu in the two sites.

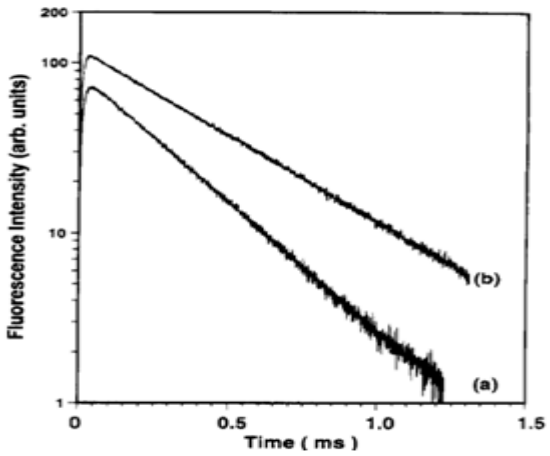

Fig 15 Fluorescence decay of $^5D_0$ of Eu^{3+} in $[EuP_5W_{30}O_{110}]^{12-}$

The fluorescence decays were single exponential at both the sites. The initial rise was due to the increase in the population from the relaxation of initially populated $^5D_1$ to $^5D_0$ state. The lifetime measured for Eu $^5D_0$ state was found to be shorter than that found in cases of Eu in usual inorganic crystals. This suggested that the encrypted cation was in contact with a water of hydration. Eu^{III} had a radiationless pathway of energy transfer from $^5D_0$ state of Eu to v=3 vibrational mode of water. Inorder to investigate the possibility of water molecule, experiments were repeated with deutarated site A occupied and in another case, both sites A and B occupied.The lifetime of deutarated sample was found to be 8 times longer than that obtained in case of sample containing H_2O. This result clearly demonstrated that Eu was attached to water molecule in the heteropolytungstates. The different lifetime of the two sites could be attributed to the different number of water molecules coordinating them. It was found that there were three water molecules coordinated to Eu at site A and two water molecules coordinated at site B. If the two sites were simultaneously occupied, then the fluorescence decay would be affected by the energy transfer between the two sites. If two Eu atoms were assumed to be encrypted within the same cluster, the Eu-Eu distance could not exceed about $5A^0$. The life ime reported for the deuterated sample did not comply with any phono assisted energy transfer. From these, it was concluded that two Eu did not occupy two different sites in the same cluster but two different sites in two different clusters.

- *Cerium Exchanged Preyssler POM:*

Cyclic Voltametric studies also showed five reversible reduction steps each involving two electrons for all $[RP_5W_{30}O_{110}]^{n-}$, over a range of 0V to -0.7V against an Ag/AgCl electrode except for $[EuP_5W_{30}O_{110}]^{n-}$ which showed four reversible steps, each involving 2,2, 4, 2 electrons, over the same potential range and against same electrode at a standard potential of -0.57 V.

- *Plutonium Exchanged Preyssler POM:*

Antonio and Soderholm obtained some truly surprising results in case of Ce-exchanged Preyssler molecule.[24] Unlike the cases of other lanthanide cations which got exchanged for the central Na^+ ion, in their +3 oxidation state under optimum conditions of time and temperature, Ce (III) showed its exchange phenomenon under extremely harsh condition. However, Ce in its +IV oxidation state, when used as starting material yielded Ce-exchanged Preyssler POM conveniently. Quite surprisingly, the CV graph of Ce-exchanged Preyssler obtained from Ce (IV) appeared to be the same as that from Ce (III) with no appearance of Ce (IV/III) reduction curve. Also, the graphs were identical with that of other lanthanide exchanged Preyssler POM (excepting Eu as said above). This problem was finally probed with the XANES technique. Cerium L2 egde XANES showed an intense sharp line 6166.5 eV for Ce(III) and a double edge resonance at 6170 eV and at 6177.5 eV for Ce(IV) in the solid state. Again, Cerium L1 egde XANES showed peaks with difference of 13 eV between Ce(III) and Ce(IV) compounds thereby, distinguishing between the two oxidation states. Surprisingly, the spectral curve as obtained from L2-edge XANES of the Ce-exchanged Preyssler POM, in solid state and in solution clearly revealed a consistency with Ce in +III oxidation state at rest potential of 0.3 V vs. SCE. Also, the peak at 6166.5 eV of L2-XANES in H_2SO_4 solution appeared to be more intense! Again, Cerium L1 egde XANES for Ce-exchanged Preyssler POM confirmedly evidenced for the presence of Ce (III). The above study thus conformed to the absence of the reduction wave in the CV studies.

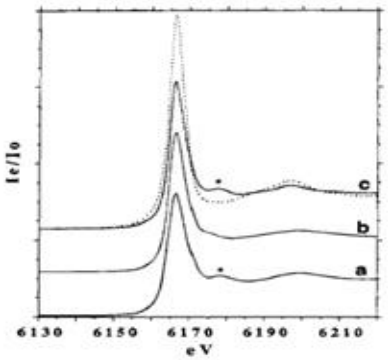

Figure 1. Cerium L_2-edge XANES for the trivalent cerium reference compounds (a) $CeTiO_3$ and (b) $CeCl_3{\cdot}7H_2O$ and (c) the cerium-exchanged Preyssler anion as the potassium salt in the solid state (solid line) and in an aqueous solution (7 mM, dashed line) of 1 M H_2SO_4 at rest potential. The vertical scale is offset for clarity.

Fig 16 XANES of Trivalent Cerium

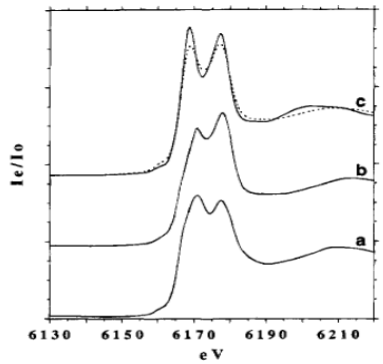

Figure 2. Cerium L_2-edge XANES for the quadrivalent cerium reference compounds (a) CeO_2, (b) $H_4Ce(SO_4)_4$, and (c) $[Ce(NO_3)_6]^{2-}$ as the ammonium salt in the solid state (solid line) and in aqueous solution (95 mM, dashed line).

Fig 17 XANES of Quadrivalent Cerium

The XANES study of Ce-exchanged Preyssler POM clearly indicated the presence of trivalent Ce cation in the cavity of Preyssler anion. The probable reason to which Antonio and Soderholm attributed the situation to is as follows:

Ammonium Cerric nitrate, $[(NH_4)_2Ce\ (NO_3)]$ contained two oxidizable NH_4^+ cations and a reducible $Ce(NO_3)^-$ anion and Ce(IV) happened to be a powerful oxidizing agent. So, in aqueous medium, Ce(IV) oxidized water to oxygen, and chloride ion to chlorine. Also it oxidized ammonia to nitrogen according to the equations:

$Ce^{IV} + ½\ H_2O \leftrightarrow Ce^{III} + H^+ + l/4O_2$
$Ce^{IV} + C1^- \leftrightarrow Ce^{III} + ½\ C1_2$
$Ce^{IV} + 1/3\text{-}[NH_4]^+ \leftrightarrow Ce^{III} + 4/3H+ + 1/6N_2$

To confirm the above reasoning, a control experiment employing the same reactants and under the hydrothermal reaction conditions excepting the Preyssler POM was performed. The reaction yielded a product with Ce in +III oxidation state. This clearly revealed that irrespective of the presence or absence of Preyssler POM, Ce (IV) was getting reduced to Ce (III) under the employed reaction conditions. However, the reason behind the more facile exchange of Ce (IV) than Ce (III) remained unanswered. Probably, the exchange of Ce(III) from $[NH_4]_2Ce^{IV}\ (NO_3)$ was pH dependent and that the aqueous solutions of ammonium ceric nitrate was highly acidic due to the hydration and hydrolysis reactions. This explanation was further supported by the pH dependent exchange of U (IV) for Na^+ in the cavity of Preyssler POM.

The difference in the normalized intensity of the XANES peak in the solid and solution phase was probably due to the protonation and hydration in the presence of H_2SO_4 which lead to a distortion in the heteropolytungstate framework of Preyssler POM thereby relocating the Ce (III) in the cylindrical cavity. Even though the cylindrical cavity of the Preyssler POM was restricted with five terminal oxygen atoms, neither the accessibility of the Ce (III) site to the solvent molecules and ions nor the possibility of the Ce ions outside the framework cavity could be ruled out. The intense XANES peak in solution may be attributed thus to the phenomenon such as a localized structural reorganization about Ce(III), bonding, hybridization, orbital mixing, etc.

- *Electrochromism and Surface Chemistry:*

$POM/PAH)_m$ multilayers, the current was found to increase linearly with the increase in the number of layers. This confirmed that equal amount of Eu-POm was deposited on each cycle. The cathodic peak potential shifted slightly to negative potential while the anodic peak slightly shifter to negative potential.

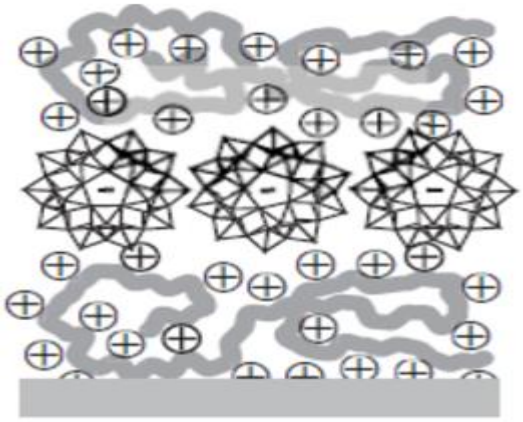

Fig 18 $[EuP_5W_{30}O_{110}]^{12-}$ in the matrix of polyelectrolyte(Top View).

The CV of $[EuP_5W_{30}O_{110}]^{12-}$ was found to consist of three peaks at -0.414 (C1), -0.481 (C2), and -0.530 V (C3) during the cathodic sweep and three peaks -0.363 (A1), -0.448(A2), and -0.498 V (A3) during the anodic sweep. The three pairs of peaks C1/A1, C2/A2, and C3/A3 corresponded to $2e^-/2H^+$ redox processes. The oxidized form of the $[EuP_5W_{30}O_{110}]^{12-}$ was found be to completely transparent while the reduced form of it showed a large absorption band at 700 nm. Furthermore, every single redox step showed an increasing coloration of the solution.

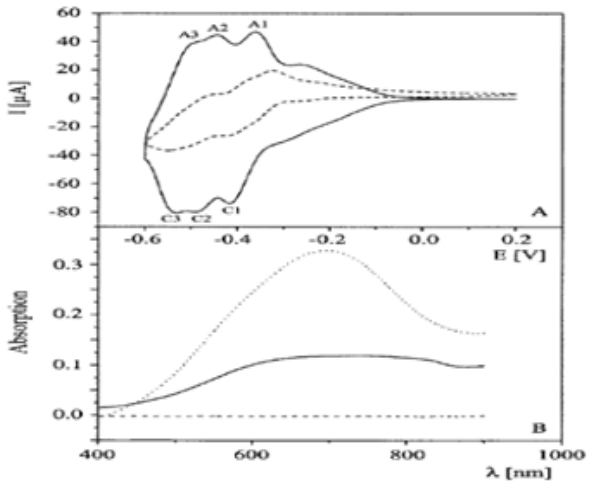

Fig 19 CV of Eu-POM and CV of (PSS/PAH/Eu-POM/PAH)$_m$ (dotted line).

✓ *The Surface Coverage Was Given By:*

$\Gamma = i_pRT\ [4 - 2\gamma t]/n^2F^2\nu A = 4i_pRT/n^2F^2\nu A$. Where, i_p was the peak current, γ is the interaction term, n was the number of electrons transferred per electroactive species, and ν is the scan rate. A was the geometric area of the electrode and all other terms have usual meaning. The average surface coverage per layer was found to be $1.47 * 10^{-10}$ mol/ cm^2 or 1.13 nm^2 per POM. The surface area from X-Ray crystallography was calculated to be 2.3 nm^2. The electrochemically determined surface coverage approximately consisted of two Eu-POM monolayers.

An optical contrast from transparent to blue revealed that the above discussed film was electrochromic. The

absorbance at 700 nm increased to 0.7 at -1.75V. For a single (PEI)/ $(PSS/PAH/Eu\text{-}POM/PAH)_{m,}$ the optical density was observed at 0.006 which was a value sufficient for practical device applications. The response time was evaluated by a double-potential step chronoamperometric experiment simultaneously while recording the absorbance of the film. A charging current was observed which decayed to zero while bleaching and to residual current while coloration. The response time was in seconds both in case of bleaching and colouration. The above experiment also confirmed the stability of the Eu-POM multilayer.

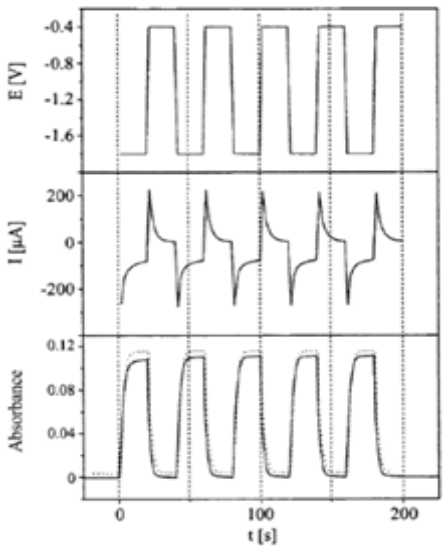

Fig 20 Absorbance at 700 nm of PEI)/ $(PSS/PAH/Eu\text{-}POM/PAH)_m$ electrode during double potential steps.

Thus the device operated reversibly with suitable response times. One year after the above report, Wang and his co-workers constructed the multilayer film by subjecting the original Na-Preyssler POM to fabrication with Polyethyleneimine(PEI) by alternative adsorption method. [28] The reason as to why PEI was employed again was perhaps because it provided various reaction sites in its primary, secondary and tertiary forms to form charge transfer complexes with heteropolytungstates. The growth process was studied using UV-VIS spectroscopy.

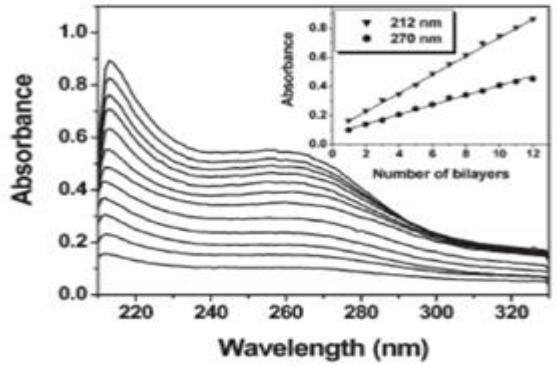

Fig 21 UV-VIS spectra of (PEI)/ $(Na\text{-}POM/PEI)_n$ with n=1-12.

The fact that Na-POM was incorporated in the multilayer film was evident from the appearance of absorbance peak at 212 nm and 270 nm which corresponded to the oxygen to tungsten charge transfer. Furthermore, the absorbance showed a linear dependence on the number of bilayer which confirmed a uniform deposition of Na-POM in deposition cycle. Likewise, FTIR supported the individual presence of Na-POM and PEI in the matrix. FTIR furnished a vibrational band at 911 cm^{-1} and 780 cm^{-1} which corresponded to $W{=}O_d$ and $W\text{-}O_c\text{-}W$ and three resolvable peaks at 1165 cm^{-1}, 1082 cm^{-1} and 1018 cm^{-1} which corresponded to $P–O_a$ stretching. Again, FTIR showed band at 1450–1600 cm^{-1} corresponding to C–C, C–N and band 2850–2950 cm^{-1} corresponding to C-H of PEI component. The band corresponding to N-H of PEI shifted from 3437 cm^{-1} to 3432 cm^{-1} indicating at the formation of hydrogen bond between the na-POM and PEI.

AFM showed a granular image texture of (PEI)/ $(Na\text{-}POM/PEI)_3$, the mean roughness of the surface being 0.530 nm over an area of 1.0 * 1.0 μm^2.

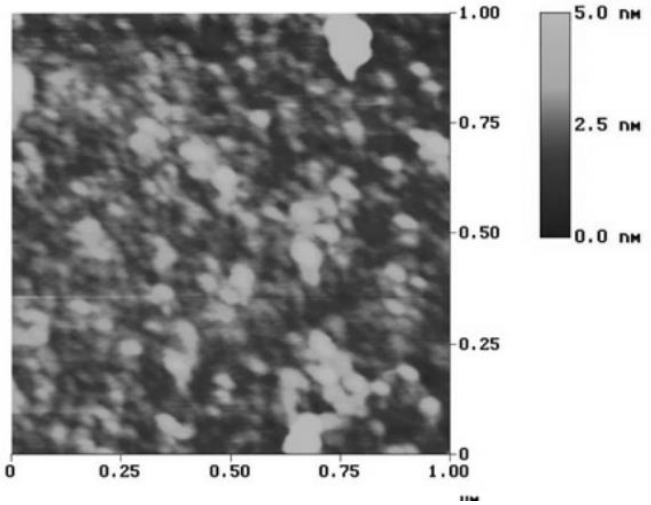

Fig 22 AFM image of (PEI)/ $(Na\text{-}POM/PEI)_3$.

The increase in the absorbance of (PEI)/ $(Na\text{-}POM/PEI)_{30}$ above 600 nm was a characteristic of reduced heteropoly blues species with the d-d charge transfer transition from W(V) to W(IV). The absorbance of the multilayer film reached saturation with UV irradiation time. Upon putting off the UV light, decoloration started occurring very fast and the bleaching process was over after 5 minutes, However, on increasing the number of bilayers from 30 to 100, the time taken for the completion of bleaching was increased to nearly 30 minutes.

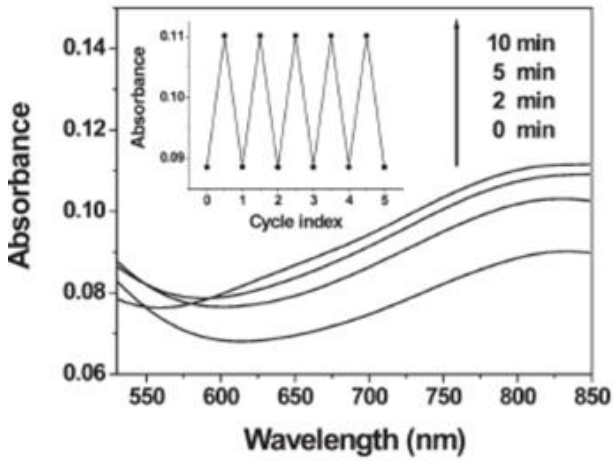

Fig 23 Plot of absorbance versus wavelength

The above graph shows reversibility in the coloration-bleaching process.

ESR (Electron Spin Resonance) studies revealed that there was no electronic change in the structure of the multilayer film before irradiation. However, after irradiation, an ESR signal for W in +5 oxidation state was obtained at room temperature. The group in question thus concluded that as a result of charge transfer from O to W in WO_6 unit, hydrogen was transferred from N of PEI to bridging O atom of photoreduced site in the WO_6 octahedral site. This caused an one electron interaction left on Oxygen atom with the proton, Simultaneously, the hole created as a result of above mentioned LMCT interacted with the non-bonding electron of Nitrogen of PEI giving rise to charge-transfer complex. The bleaching was caused by a back reaction prompted from a charge transfer from W (V) to oxygen molecule. XPS (X-ray photoelectron studies) which indicated at the presence of W (V) in the irradiated also agreed with the ESR results.

When the film with Na-POM as the outermost layer was irradiated with UV light, there was change observed in ζ- potential. Whereas, when PEI was the outermost layer, a reduction in the value of ζ- potential was observed. The ζ-potential decreased gradually with the increase in the UV exposure time and after 15 minutes of UV irradiation, the ζ-potential decreased from +69 mV to -71 mV after which the changes became saturated. XPS measurement revealed that when the outermost layer was Na-POM, two intensity peaks were obtained whereas, when the outermost layer was PEI, a negative shift from the above peaks were observed due to the core level shift owing to the adsorption of PEI. For $(PEI/Na\text{-}POM)_{30}$/PEI film whose ζ- potential decreased from +69mV to -71 mV after 15 minutes of UV irradiation showed peaks at position similar to that in case of NaP_5W_{30}. This clearly put forward that the surface of $(PEI/Na\text{-}POM)_{30}$/PEI was same as that of NaP_5W_{30} after UV irradiation, This agreed with the inversion of ζ- potential observed.

QCM measurements were also performed to study the effect of UV radiation on $(PEI/Na\text{-}POM)_{30}$/PEI film. The mass of the multilayer substrate could be determined from Sauerbrey equation:

$$\Delta F = -\frac{2F_o^2}{A\sqrt{\mu p}}\Delta m$$

Where F_o= frequency of the sensor; A=area of the electrode; μ = shear stress of the quartz; ρ= the specific gravity of the quartz.

In the fabrication process of $(PEI/Na\text{-}POM)_{30}$/PEI film, adsorption of one layer of PEI and of Na-POM individually resulted in a decrease in the frequency and an increase in the weight of the film. The packing density estimated from the increase in the weight was almost the same as the crystal packing. The frequency upon 15 minutes of UV irradiation on $(PEI/Na\text{-}POM)_{30}$/PEI with PEI as the outermost layer, was equivalent to that of the disappearance of one PEI layer. XPS and QCM studies thus allowed one to conclude that the UV irradiation caused a detachment of the outermost PEI layer thereby exposing the underlying NaP_5W_{30}. Hence the inversion in ζ- potential. The photochromic reaction occurred as follows:

Scheme 1

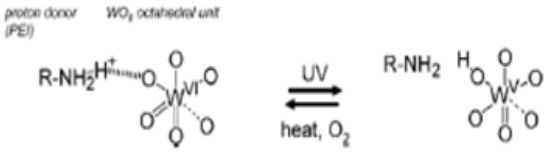

The transfer of protonated hydrogen broke the electrostatic bonds and weakened the ionic strength of PEI. Thus the interface electrostatic interaction between PEI and Na-POM became weaker and therefore the outermost PEI layer got detached. Immmersion in high concentration salt might also result in elimination of electrostatic interaction in the multilayer film due to the increase in entropy. Thus PEI, being in equilibrium in aqueous solution was easier to detach. The above may be attributed to consideration of Na-POM as the bulk layer due to the high packing density. The electrostatic interaction between PEI and NA-POM which disappeared during photochromism, got generated while due to the further hydrogen bonding. Hence the film was stable still. Thus, it can be concluded that photochromism weakened the interaction between PEI and Nap_5W_{30} and made the outermost layer unstable, thereby leading to the detachment of PEI layer. The multilayer film from which the detachment of PEI resulted from UV irradiation was further dipped in PEI solution and subjected to ζ- potential measurement. A decrease to -72mV was recovered to a value of +55mV, which was same as the initial value of before the detachment of PEI layer. Thus the switching of the ζ- potential and hence the reversible control of the surface properties were made possible.

A communication in 2010 revealed photoswitchable fluorescence from the inorganic hybridized nanostructure based on the alternative adsorption of negatively charged NaP_5W_{30} or CdSe@CdS nano particles and the positive-charged PEI.[30] Now while, $(PEI/Na\text{-}POM)_{10}$ showed a strong UV light absorption in the region of 550-800 nm, $(PEI/CdSe@CdS)_{10}$ showed a strong fluorescence peak in the region of 550-650 nm which coincided with the wavelength range of photochromism of $(PEI/Na\text{-}POM)_{10}$. Thus if luminescent CdSe@CdS nano particles and Na-POM were allowed to combine in the same nanostructure with a distance of less than 10 nm in between them, Fluorescence Resonance Energy Transfer (FRET) would be expected to occur between the nanoparticles and the photochromic Na-POM, thereby giving rise to fluorescence switching. The efficiency of the fluorescence switching was optimized by altering the number of layers of Na-POM and the fluorescence intensity was optimized by altering the number of composite layer.

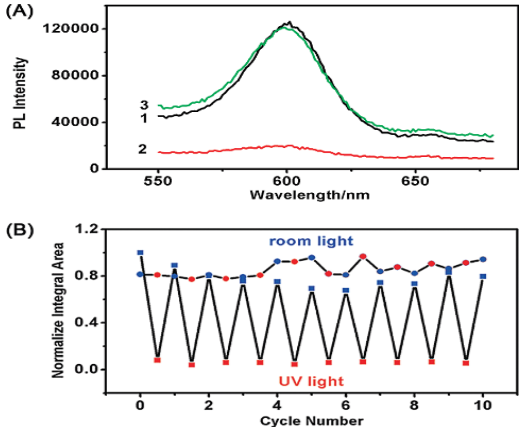

Fig 24 (A)Fluorescence switching of $[(PEI/Na\text{-}POM)_9/PEI/CdSe@CdS)]_{10}$ film to UV exposure (B) Normalized integral fluorescence area of $[(PEI/Na\text{-}POM)_9/PEI/CdSe@CdS)]_{10}$ film in the

✓ *UV-Vis Cycles As A Function Of Cycle Number:*

Thus it was found that a strong fluorescence peak existed at 600 nm. Upon exposure to UV irradiation, the fluorescence started getting quenched. Upon further exposure of the UV irradiated multilayer to room light, the fluorescence got recovered to 90% of the original value after 24 hours. On increasing the intensity of room light, the time of recovery decreased. The photoswitchable Fluorescence of the $[(PEI/Na\text{-}POM)_9/PEI/CdSe@CdS)]_{10}$ in both their 'on' and 'off' states were found be highly reversible and stable. The interlayer distance was found to fall in the effective range of energy or charge transfer. The occurrence of fluorescence switching or the FRET mechanism might be explained as below:

When the $[(PEI/Na\text{-}POM)_9/PEI/CdSe@CdS)]_{10}$ was irradiated with UV light, a ligand to metal charge transfer from the low lying 2p orbital of oxygen occurred to the high level d-orbital orbital of Na-POM. This one electron in the d-orbital absorbed visible light via intervalence charge transfer among metal centers and d-d transitions in the region of 550-800 nm. Since the CdSe@CdS nanoparticles fluoresced in the same region as the reduced Na-POM, the fluorescence of the nanostructured composite got quenched. When the $[(PEI/Na\text{-}POM)_9/PEI/CdSe@CdS)]_{10}$ was placed at room light, the resonance energy transfer from the nanoparticles to Na-POM got interrupted and the fluorescence got recovered.

Meanwhile in 2004, Dong and his co-workers. prepared multilayer thin film nanocluster out of Preyssler POM via the Layer-by-Layer (LBL) mechanism. [31] The nanocomponent incorporated on their surface was Fe_3O_4 coated with poly (diallyldimethylammonium chloride) (PDDA) (PDDA: Fe_3O_4). The nano-components were important because of the high surface area to volume ratio which had its basis on the special sensor effect and also from the electrochemical point of view. The multilayer thin film derived from P_5W_{30} solution in 0.1 M H_2SO_4 reduced HNO_2 and IO_3^- and showed Hydrogen evolution Reaction(HER) in acid media. The latter made them durable hydrogen cathode component for fuel cell.

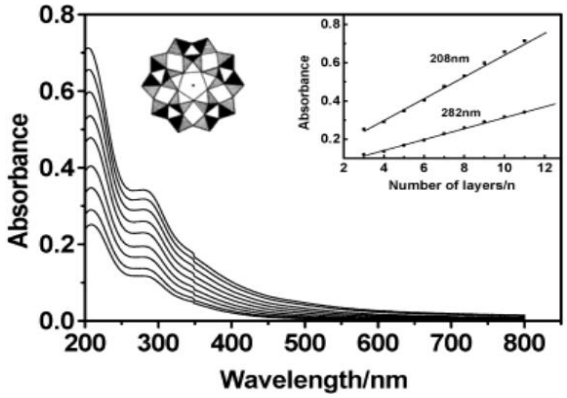

Fig 25 UV-VIS absorption spectra of the thin film of Preyssler POM

The UV-VIS absorption spectra helped to characterize the growth process of the multilayer thin film. The P_5W_{30} being the outermost layer absorb at the same wavelength as the sequential deposition. The absorbance at 208 nm and 282 nm corresponding to the charge transfer from oxygen to tungsten increased linearly with the thickness of the layer. This linear dependence of absorbance on the thickness of the multilayer indicated at the construction of a uniform multi-layer film by the POM.

The X-ray Photoelectron spectroscopy showed two peaks at 35.0 eV and at 37.2 eV corresponding to the 4f orbital of tungsten. The Peak at 132 eV corresponded to 2P orbital of Phosphorous. And the peak at 710.2 eV corresponded to the $^2P_{3/2}$ of Fe. Thus XPS clearly indicated at the presence of Fe_3O_4 nanoparticles and P_5W_{30} in the multi-layer. The 4-aminobenzoic acid (4-ABA) containing a –COOH group modified with Glassy carbon electrode (GCE) was alternatively immersed in P_5W_{30} and PDDA: Fe_3O_4 solution. The multi-layer thin films of P_5W_{30} were assembled by dissolving in 0.1 M H_2SO_4 solution. The 4PDDA:Fe3O4/5P5W30/PDDA/4-ABA/GCE exhibited four redox couples waves with the formal potentials (E_f) of -0.26, -0.33, -0.39, and -0.59 V, respectively, the pattern being different from that of P_5W_{30} in 0.1 M H_2SO_4 solution at a bare GCE.

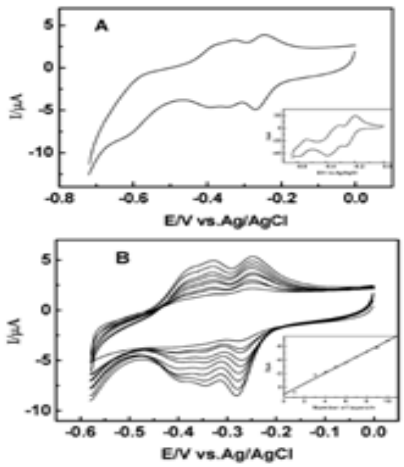

Fig 26 CV of the above compound

The cyclic voltammetry of P_5W_{30} in 0.1 M H_2SO_4 show two four-electron redox waves each at -0.23V and at 0.35 V. The CV of the five layered P_5W_{30} in 0.1 M H_2SO_4 show two redox waves at 0.33V and 0.39V, each coming from the second four electron redox wave of the previous case. The second redox wave of P_5W_{30} splits into two redox waves in the case of the latter because the electrostatic interaction between the P_5W_{30} and PDDA: Fe_3O_4 influenced the redox transfer and caused the split to occur into a two transfer process. Since the last redox wave is complicated by the overlap with the Hydrogen evolution reaction, the first three redox waves were used to monitor the multi-layer deposition. Thus a good linear relationship between the layer number and the first cathodic peak was obtained. The second CV demonstrated uniformity in the growth of the P_5W_{30} film. Furthermore, it was found that with the increase in the number of the layers, a negligible shift in the formal potential was observed. This clearly indicated that no electrochemistry was exhibited by the PDDA: Fe_3O_4. Thus, the electrochemistry of P_5W_{30} contributed to the electrochemistry of PDDA: Fe_3O_4/P_5W_{30} composite layer. This also pointed out that Fe_3O_4: PDDA layer acted as a conductive nano- layer without affecting the electron transfer of P5W30 sandwiched between them. Again, the cyclic voltammetry of PDDA:

Fe_3O_4/P_5W_{30} showed chemically reversible surface redox chemistry. The cathodic and anodic peaks showed linearity with the scan rate upto 289mV. The ratio of anodic peak to cathodic peak was found to be unity at all scan rates. All these results were consistent with the electrochemical behavior of the surface-confined POMs. The surface coverage of the POM was given by:

$\Gamma = i_pRT\ [4 - 2\gamma t]/n^2F^2\nu A = 4i_pRT/n^2F^2\nu A$. Where, i_p is the peak current, γ is the interaction term, n is the number of electrons transferred per electroactive species, and ν is the scan rate. A is the geometric area of the electrode and all other terms have usual meaning. The surface area of the POM was found to be 4.00 nm^2 and corresponded to a submonolayer.

A.A. Tarlani et al. studied the immobilization of Preyssler Heteropolyacid (HPA) on functionalized silica via chemical bonding to aminosilane groups according to the following scheme: [32]

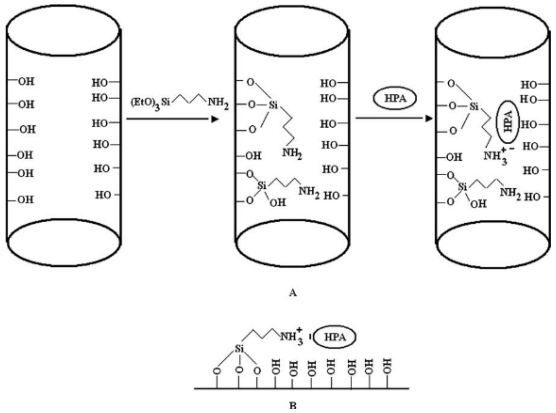

Fig 27 Immobilization of Preyssler Heteropolyacid (HPA) on functionalized silica

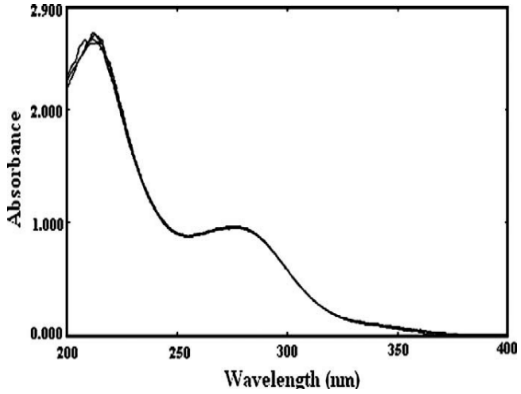

Fig 27 The absorption spectra of Preyssler HPA immobilized on functionalized silica

The silica material did not show any tendency of adsorbing the HPA prior to grafting with amine ligand. Thus the Infra-red spectra showed no characteristic peak of HPA of bare silicas that were impregnated with HPAs and then washed with water. The HPA after contact with silica remained intact in solution as confirmed by ^{31}P NMR. The surface area of functionalized silica decreased upon immobilization of HPA on it due to the filling of the pores. Thus the lower loading of Preyssler HPA was ascribed to the small pore size of silica and larger size of Preyssler cluster. The strong interaction between the silica and the immobilized Preyssler HPA make them suitable homogeneous catalysts.

Kurth and Faul and their co-workers in 2009 further employed $[EuP_5W_{30}O_{110}]^{12-}$(EPW) and a variety of organic surfactants of varied alkyl chain lengths to develop hybrid nanostructures via Ionic Self Assembly (ISA). [33] FTIR recorded the asymmetric and symmetric stretching frequencies of the all the alkyl chains employed. The slight shift in the frequencies of EPW suggested that the POMs were organized in the presence of the positively charged surfactant. Two strong absorption bands at 201 nm and at 280 nm explained the incorporation of EPW in the matrix of

surfactant without structural disintegration. TGA revealed different degradation temperature for different surfactant encapsulated POMs (SEPs). DSC studies of the various SEPs to conclude that with the decrease in the length of the alkyl chain, the transition temperature and the transition enthalpies also decreased. This further indicated at the structural rearrangement rather than at the phase change of the cluster. X-ray scattering investigation further evidenced for the conformational order of the surfactant. Thus, while certain spacing calculated indicated at the close spacing of the alkyl chains(but not crystalline), certain spacing values(like in case of ferrocene containing surfactants) indicated at the loose spacing. To prove that the structures were isomorphous, certain simple calculations were performed. In case of EPW/C_nDA (DA=dimethlammonium bromide) the d-spacing showed a good linearity with the length of the chain and the dependence was equated as: d_n=0.142n+1.27 (nanometers). The slope ($\Delta d/\Delta n$) and intercept of the equation gave the contribution of alkyl chain and EPW layer plus the surfactant headgroup to the bilayer thickness (d_n), respectively. The tilt angle, α was calculated34.0^o from the relation 0.254sin $\alpha = \Delta d/\Delta n$. Thus the thickness of the inorganic EPW layer was estimated from the intercept minus the contribution from the surfactant headgroup.

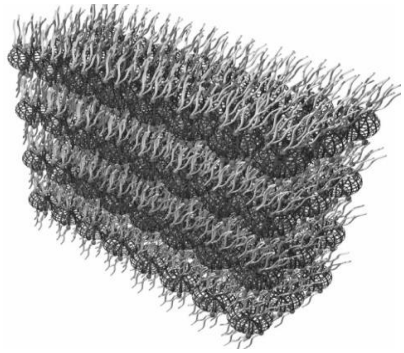

Fig 28 EPW/CnDA complexes showing interlocked and tilted surfactant alkyl tails

Thus the very little difference in the small angle X-ray scattering pattern revealed that the structure were isomorphous. The compounds as-prepared were investigated under polarized optical microscope and were found to be thermotropic liquid crystals at room temperature. They also showed the existence of lyotropic phase behavior.

The excitation spectra of EPW solid, (a), EPW/C_{16}DA solid (b), and EPW/C_{16}DA film (c) exhibited series of sharp lines that corresponded to the characteristic transitions of Eu^{3+}. The broad band in between 240 to 350 nm due to the ligand to metal charge transfer in EPW solid was found to be missing in the spectra generated. The reason was laid as: the hopping of d^1 electron over the lattice created a quenching channel against the energy transfer from the LMCT states to emitting levels of Eu^{3+} due to the easy recombination of the one d electron and the hole.

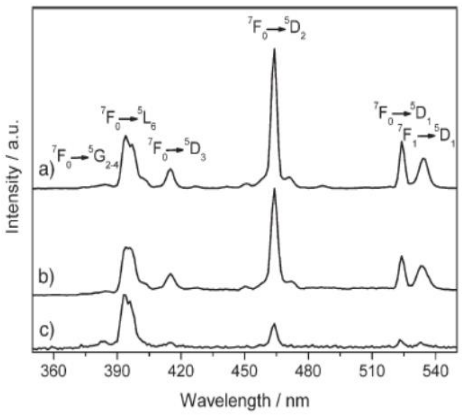

Fig 29 Excitation spectra of (a) EPW solid (b) EPW/C_{16}DA solid and(c) EPW/C_{16}DA film

As discussed above, Kurth previously substantiated the elctrochromism of EPW anion. A new broad band appeared in case of EPW/C_{16}DA upon application of a potential more negative than -0.9V. With the increase in the degree of reduction, the colour intensified. During the optical scanning in between -0.9V to -2.2V, a change from transparency to blue was observed which confirmed eletrochromism. However, the ferrocene containing EPW-surfactant did not show any light absorbing property upon application of reduction potential in any range. This might be attributed to the donor-acceptor interaction between EPW and ferrocene.

➢ *Catalysis:*

Preyssler POM has contributed the maximum in the field of catalysis perhaps because it satisfies much as a green catalyst. The effort for the continuous search of the cleaner, environment friendly and less hazardous catalyst lead the researchers to seek into the Preyssler heteropolytungstates with promising catalytic activity, efficiency and selectivity. With 14 Bronsted acidic protons, Preyssler HPA functioned as a very good Bronsted acid. Furthermore, the Preyssler catalyst could be recycled and reused several number of times without loss in its activity. Herein, we list the organic reaction which had been conveniently catalyzed by Preyssler catalyst:

- *Esterification of Phthalic Anhydride With 1-Butanol And 2-Ethylhexanol:*

The esterification reaction was optimized for time and percentage conversion by using the various heteropolyacids.[36] H14 [P5W30O110] and H14[P5W29MoO110] were found to exhibit the higher yields perhaps due to the highest number of acidic protons. In fact, when one of the tungsten atom from the original Preyssler POM was replaced with one Molybdenum, the resulting heteropolyacid seemed to exhibit the highest yield of 100%. While performing the esterification reaction with Mo substituted Preyssler POM, the solution turned to blue from green which indicated the reduction of Mo(V) to Mo(VI) and a consequent increase in the acidity. Ester decomposition of dioctyl phthalate by the various heterpolyacids were also recorded. The trend was observed to be similar to the esterification reaction, i.e., Preyssler type POM exhibited greater activity than Keggin and Dawson HPAs. The replacement of one W by one Mo perhaps

resulted in distortion of the structure with a consequent increase in the activity of the acid catalyzed reaction.

- *Protection of Alcohol Using 3,4-Dihydro-2-H-Pyran:*

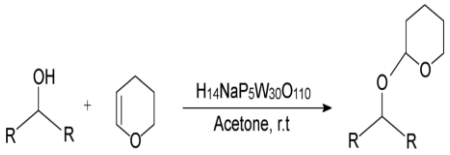

The presence of the Preyssler catalyst allowed mild reaction conditions, short time, high yield and high efficiency. [37]

- *Epoxidation of Olefins Using Peroxide:*

In the epoxidation of olefins using H2O2, Keggin POM due to the low hydrolytic stability could not suitably catalyse the aforesaid reaction.[38] Thus, employing a phase transfer catalyst or a different hereropoly acid was an alternative. In this reaction, the Preyssler anion was isolated using a large isopolycation Al37+. The Preyssler HPA showed macroporous structure and low surface areas. However, BET surface area of the as-prepared catalyst, i.e., [Al13O4(OH)24(H2O)12]2[NaP5W30O110] showed mesoporous character with a moderate value which was attributed to equality of cation-anion charges and their huge sizes. DTA curve showed endothermic peaks, the behavior being similar to that of zeolite. Besides being thermally stable, the Preyssler POM was hydrolytically stable too due to the large cluster assembly energy.

- *Synthesis of Substituted 2-Amino-4H-Chromenes:*

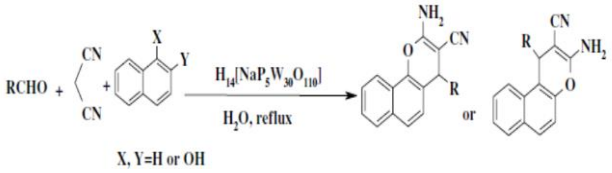

In addition to the use of green catalyst, greener and cleaner solvent, i.e, water was used for the above reaction. [39]

- *Direct Esterification of Butanol:*

The esterification reaction of butanol in various solvent with the various Preyssler type POMs were performed. The reaction with dicloroethane as solvent gave the best yield.[40] The choice of the solvent depended on the interaction of the polarized polyoxoanion with the solvent to place the m.o. energies at appropriate level or to lower the activation energy. Molybdenum substituted Preyssler POM was observed to furnish the maximum yield of 100% in 4 hours with dichlroethane as the solvent. Two pathways were possible for the reaction: (1) oxidation of butanol to butanoic acid by H_2O_2 in the presence of Preyssler catalyst followed by catalytic esterification. (2) oxidation of butanol to butanal followed by formation of hemiacetal and its subsequent esterification. The acidity of Preyssler POM makes the first path more appropriate.

- *Synthesis of 1,5-Benzodiazepines In Refluxing Ethanols:*

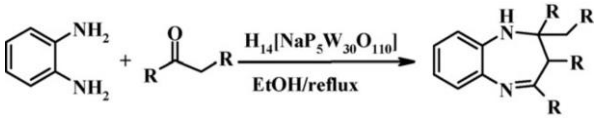

The reaction with Preyssler catalyst occurred took shorter time to finish than the reaction with Keggin catalyst. [41]

- *Acetylation of Alcohols, Phenols, Salicylic Acids In Acetic Anhydride:*

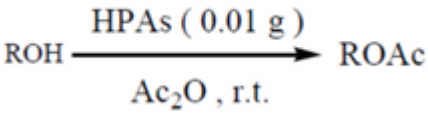

Preyssler POM gave the maximum yield.[42]

- *Deamination of Some N-Amino Nitrogen Heterocycles:*

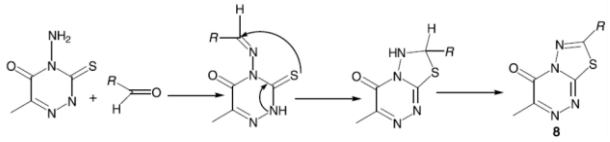

Scheme1

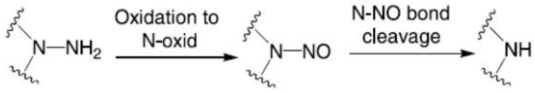

Scheme 2

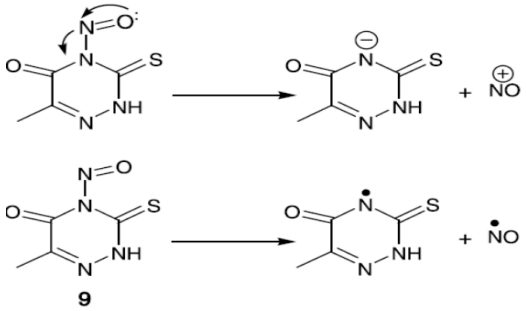

Scheme 3. [46]

- *Synthesis of 4(3H)-Quinazolinones Under Ultra-Sonic Irradiation Using Silica-Supported Preyssler Nano Particles:*

The quilazolinones were an important class of compounds from the biological point of view and their synthesis under ultrasonication using an HPA promised good results.[47] Due to the increase in the activity of nano particles, development of catalyst of low dimension had been much focused on. The novel properties of nanochemistry were combined with the goodness of Preyssler catalyst and silica supported Preyssler POM was employed for the aforesaid synthesis.

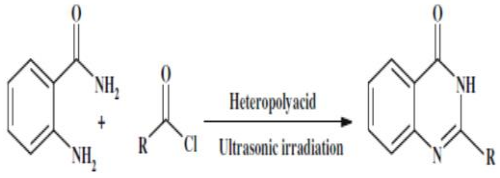

Scheme 1.

TEM and IR showed that the Preyssler anion remained intact on the silica surface. With Preyssler nanoparticles, the reaction furnished the product in best yield and selectivity.

- *Synthesis of Bis(Indoyl)Alkanes Under Ultra-Sonic Irradiation Using Silica-Supported Preyssler Nano Particles:*

Bis(indonyl)alkane is known to control estrogen metabolism and prevents cancer.

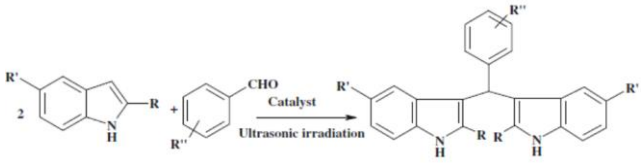

The novel properties of nanochemistry were combined with the goodness of Preyssler catalyst and silica supported Preyssler POM was employed for the aforesaid synthesis. [48]

- *Photodegradation of Methyl Orange Under UV Light Using H_2O_2 As An Oxidant:*

The silica supported Preyssler nano structure was obtained through micro-emulsion method and was characterized using TEM.[49] The TEM, PXRD and IR all confirm that the Preyssler structure remained intact on the surface of the silane without ant change. The degree of methyl orange decolorization was interpreted as an effect of photocatalytic activity. The reaction conditions was optimized using Preyssler acid as the standard catalyst and the photodegradation of the methyl orange was measured at various pH of 1.0, 2.0 ad 3.0. the degree of methyl orange decolorization indicated at the excellent photocatalytic activity of Preyssler acid. The lower pH was favourable for decolorization by the Preyssler catalyst.

- *Protection of Carbonyl Compounds:*

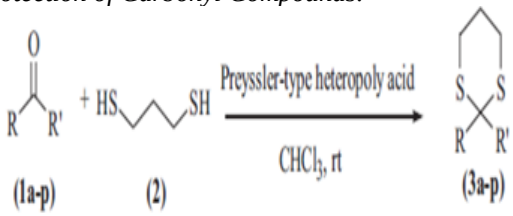

The optimization of the reaction conditions revealed that that Preyssler catalyst in just 0.1 mol% and optimum time yielded the best result. [62]

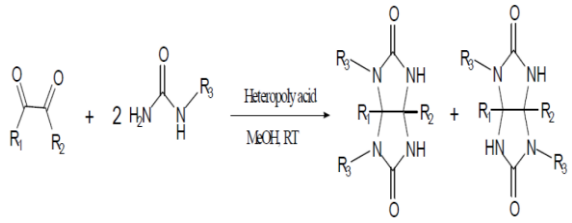

Both Well-Dawson and Preyssler catalyst furnished the best result with a conversion of 100%.

- *Synthesis of Diphenylmethyl Ethers (DPME): [63]*

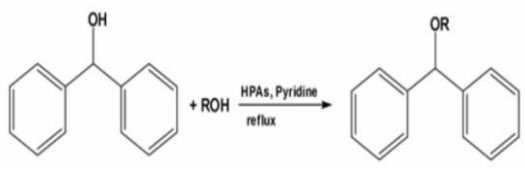

- *Synthesis of Calix[4]Pyrroles: [64]*

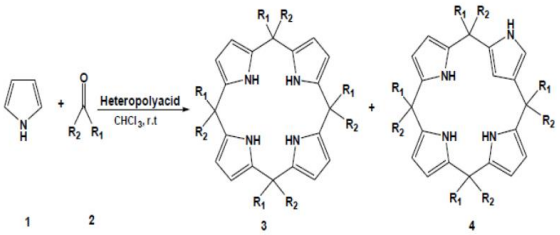

VII. CONCLUSION

One Serendipity and Preyssler POM really did not really pause to allow inorganic chemists to come up with interesting results. The architectural relevance and the electroactivity of the Preyssler POM attracted the attention of renowned scientists like MT Pope, Antonio, Soderhelm, Poblet etc. who suitably exploited and elucidated the aforesaid system. Preyssler heteropolytungstates had thus been noted to have marked contribution in the field of electrochemistry, catalysis and medicine. The doughnut shaped heteropolytungstate was the first example of POM with an internal cavity within. The initially encrypted sodium cation at the centre could be replaced with trivalent lanthanide cations and few alkaline earth metals under vey harsh conditions. The position of the encapsulated cation varied as a function of the ionic radii of the same.This also caused a change in the symmetry point group pf the entire system. The replacement of the central sodium ion with a number of lanthanides and other cations furnished new properties and chemistry which were readily explored. The surface chemistry of this Preyssler POM had much been exploited via the layer-by-layer mechanism, Ionic Self-Assembly method, multi layer composites and nano composites etc. They had also been observed to act as building precursor for construction of extended POMs. The Preyssler POM and its derivatives were subjected to a number of instruments and techniques for the apt conveyance of the results.

ACKNOWLEDGEMENTS

In fact, we set on to collectively survey the Preyssler system with an intention to search for the lacuna in this region and to make for it! Thus, even though, a number of informative drafts were reported on electrochemistry, XANES and theoretical calculations, surface and catalysis, very less reports on linking and extended structure exist. This situation is perhaps through the very many challenges met in obtaining a single-crystal of high quality for the Preyssler-based compounds. Example, lanthanide owing to very high affinity for oxygen rich surfaces like that of Preyssler compound react very fast with it leading to precipitation. Thus, obtaining a single crystal goes in vain! In addition, there has been no such report of capping of Preyssler POM or employing any supramolecular compound for obtaining modified structure. A study on deriving ferrocene derivative of Preyssler has never been reported.A lot like studies that have been carried out by our group with other POM system like that of Anderson, and Lindqvist etc. has never reported for the Preyssler system. Our group is keen to explore such aspects and establish more chemistry of Preyssler POM. Thus the above perspectives are in keeping with not just the published works of the region but to familiarize the aspirants with its unpublished aspects too.

REFERENCES

[1]. A.Müller, F.Peters Chem. Rev. 98(1998) 239
[2]. D-L Long, E. Burkholder, L. Cronin, Chem. Soc. Rev. 36(2007) 105
[3]. N.Kharat ,M. Abedini,Transition Metal Chemistry 28 (2003) 339
[4]. M. H. Alizadeh, S. P. Harmalker, Y. Jeannin, J. MFrBre, M. T. Pope ,J. Am. Chem. Soc. 107 (1985) 2662
[5]. K-C Kim, M. T. Pope, G. J. Gama, and M.H. Dickman, J. Am. Chem. Soc 121 (1999) 11164
[6]. Z-M Zhang, S. Yao, Y-G Li, X-B Han, Z-M Su,Z-S Wang, and E-B Wang Chem. Eur. J. 18, (2012) 9184
[7]. M. S. Kaba, I. K. Song, D. C. Duncan, C. L. Hill, M. A. Barteau Inorg. Chem. 37(1998) 398
[8]. M. H. Dickman, I. Gennaro, J. Gama, K-C Kim, M. T. Pope, Journal of cluster science.. 7(1996)
[9]. C.M. Granadeiro, B. de Castro, S. S. Balula, L. C-S, Polyhedron 52 (2013) 10
[10]. Y. Lu, Y. Li, E. Wang , X. Xu, Y. Ma,Inorganica Chimica Acta 360 (2007) 2063
[11]. Qin, X-Z Song, S-Q Su, S. Dang, J. Feng, S-Y Song, Z-M Hao, H-J Zhang, Dalton Trans., 41 (2012) 2399
[12]. Inorg. Chem. 2006, 45, 761-766, Firasat Hussain,† Ulrich Kortz,*,† Bineta Keita,‡ Louis Nadjo,*,‡ and Michael T. Pope
[13]. Z. Zhang, S. Yao, Y. Qi, Y. Li, Y. Wang and E. Wang Dalton Trans. (2008) 3051
[14]. X. Wang , J. Li, A. Tian, H. Lin, G. Liu, H. H. Wang , J. Li, A. Tian, H. Lin, G. Liu, H. Hu Inorganic Chemistry Communications 14 (2011) 103.
[15]. C-Y Yang,L-CuiZhang , Z-J Wang, LinWang, X-HuiLi,Z-M Zhu, Journal of Solid State Chemistry 194 (2012) 270
[16]. H. E-Hosseini, M. Mirzaei J Clust Sci 23 (2012)345
[17]. Y-Y Li,J-W Zhao, Q. Wei, B-F Yang, H.He,G-Yu Yang, Chem. Asian J. DOI: 10.1002/asia.201301305
[18]. M-X Liang, C-Z Ruan, D. Sun, X-J Kong, Y-P Ren, L-S Long,R-B Huang, and L-S Zheng Inorg. Chem. 53(2014) 897
[19]. I Creaser, M. C. Heckel, R. J. Neitz, and M. T. Pope, Inorg. Chem. 32(1993) 1573
[20]. K. Takahashi, T.Sano, M. Sadakane, Z. Anorg. Allg. Chem. 640 (2014) 1314
[21]. Ming-Hsi Chiang, Mark R. Antonio* and L. Soderholm, DaltonTrans,(2004) 3562
[22]. L. Soderholm, M. R. Antonio, S. Skanthakumar, and C. W. Williams, J. Am. Chem. Soc. 2002, 124
[23]. L. Soderholm, G. K. Liu, J. Muntean, J. Malinsky, and M. R. Antonio ,J. Phys. Chem. 99(1995) 9611
[24]. M. R. Antonio, L. Soderholm, Inorg. Chem. 33(1994) 5988
[25]. M. R. Antonio, L. Soderholm, C. W. Williams, N. Ullah,L. C. Francesconi J. Chem. Soc., Dalton Trans.(1999) 3825
[26]. M. R. Antonio* and M-H Chiang, Inorg. Chem. 47(2008) 8278
[27]. B.S. Liu, D. G. Kurth, H. Möhwald, D. Volkmer Adv. Mater. 14(2002)
[28]. M. Jiang, E. Wang, G. Wei, L. Xu, Z. Kanga Z. Lib New J. Chem. 27(2003)1291
[29]. Y. Nagaoka, S. Shiratori, Y. Einaga, Chem. Mater. 20(2008) 4004
[30]. B. Qin, H. Chen, H. Liang, L. Fu, X. Liu, X. Qiu, S. Liu, R.Song, Z.Tang, J. Am. Chem. Soc. 132 (2010) 2886
[31]. M. Huang, L. Bi, Y. Shen, B. Liu, S. Dong, J. Phys. Chem. B 108(2004) 9780
[32]. A.Tarlani , M. Abedini , A. Nemati , M. Khabaz , M. M. Amini, Journal of Colloid and Interface Science 303 (2006) 32–38
[33]. B.T. Zhang, S. Liu, D. G. Kurth, C. F. J. Faul ,Adv. Funct. Mater. 19(2009) 642
[34]. S. Sharet, E. Sandars, Y. Wang, O. Zeiri, A. Neyman, L. Meshib, I. A. Weinstock, Dalton Trans. 41(2012) 9849
[35]. L. Ning, W. Zhang, H. Yan, H. Pang, H. Ma, Y. Yu, Journal of Colloid and Interface Science 403 (2013) 91
[36]. M. Arabi , M. M. Amini , M. Abedini ,A. Nemati , M. Alizadeh Journal of Molecular Catalysis A: Chemical 200 (2003) 105
[37]. N. Feizi, H. Hassani, M. Hakimi, Bull. Korean Chem. Soc. 26 (2005) 2087
[38]. A.N. Kharat, M. M. Amini, M. Abedini React.Kinet.Catal.Lett. 84 (2005) 37
[39]. M. M. Heravi, K. Bakhtiari,V. Zadsirjan,F.F. Bamoharram, O.M. Heravic Bioorganic & Medicinal Chemistry Letters 17 (2007) 4262
[40]. F. Bamoharram, M.M. Heravi,M.R, M.Jahangir, A.Gharib ,Journal of Molecular Catalysis A: Chemical 271 (2007) 126
[41]. M. M. Heravi, F.Derikvand,L. Ranjbar, F.F. Bamoharram Journal of Molecular Catalysis A: Chemical 261 (2007) 156

[42]. M. M. Heravi, F. K. Behbahani, F. F. Bamoharram, ARKIVOC xvi (2007) 123
[43]. M.H. Alizadeh, T.Kermani, R. Tayebee, Monatshefte für Chemie 138(2007) 165
[44]. R. Hekmatshoar , S. Sajadi , M.M. Heravi, F. F. Bamoharram, Molecules 12 (2007) 2223
[45]. Gharib, M. Jahangir, M. Roshani, 12th International Electronic Conference on Synthetic Organic Chemistry (ECSOC-12) 1-30 November 2008
[46]. M. M. Heravi, S.Sadjad, R.Hekmatshoar, H. A. Oskooie, F. F. Bamoharram, Monatshefte für Chemie 139 (2008) 107
[47]. M. M. Heravi, S. Sadjadi, S. Sadjadi, H. A. Oskooie, F. F. Bamoharram Ultrasonics Sonochemistry 16 (2009) 708
[48]. M. M. Heravi , S.Sadjadi, S.Sadjadi, H. A. Oskooie, F.F. Bamoharram Ultrasonics Sonochemistry 16 (2009) 718
[49]. F.F. Bamoharram, M.M. Heravi, M. Roushani, M.R. Toos, L.Jodeyre, Department Green Chemistry Letters and Reviews 2(2009) 35
[50]. A.Gharib, M. Jahangir, M.Roshani, Efficient Catalytic Synthesis of primary Carbamates using Preyssler heteropolyacid catalyst, $H_{14}[NaP_5W_{30}O_{110}]$ under solvent-free and in Green conditions 13th International Electronic Conference on Synthetic Organic Chemistry (ECSOC-12) 1-30 November 2008
[51]. A.Gharib, M. Jahangir, M.Roshani, Efficient Catalytic Synthesis of Pyrazolo[3,4-d]pyrimidine, Pyrazolo[4,3-e][1,2,4]triazolo[1,5-c]pyrimidine, Pyrazolo[4,3-][1,2,4]triazolo[1,5-c]pyrimidine, Pyrazolo[3,4-d]pyrimidin-4-one derivatives using Heterogeneous Preyssler Heteropolyacid, H14[NaP5W30O110]/SiO2 13th International Electronic Conference on Synthetic Organic Chemistry (ECSOC-12) 1-30 November 2008
[52]. A.Gharib, M. Jahangir, M.Roshani, Catalyzed N-acylation of carbamates and oxazolidinones by Heteropolyacids (HPAs) 13th International Electronic Conference on Synthetic Organic Chemistry (ECSOC-12) 1-30 November 2008
[53]. Heravi, M. Majid, Sadjadi, S. Hekmatshoar, R.Oskooie, A.Hossein, F.F. Bamoharram Chinese Journal of Chemistry 27(2009) 607
[54]. G.P. Romanelli,D.M. Ruiz, J.C. Autino, H. E. Giaccio, Mol Divers 14 (2010)803
[55]. F.F. Bamoharram, Molecules 15(2010) 2509
[56]. M. Rahimizadeh, G. Rajabzadeh, S-Mola Khatamia, H. Eshghia, A. Shiri,Journal of Molecular Catalysis A: Chemical 323 (2010) 59
[57]. M.M. Heravi, N. T-Hoseini and F. F. Bamoharram Green Chemistry Letters and Reviews 3 (2010) 263
[58]. F.F. Bamoharram , M. M. Heravi ,P. Ardalan , T. Ardalan Reac Kinet Mech Cat 100 (2010) 71
[59]. A.Gharib, M. Jahangir, M. Roshani, J. (H) W. Scheeren, Bulgarian Chemical Communications, 42, (2010) 210
[60]. A.Gharib A,M. Jahangir M. Roshani , J. (H) W. Scheeren,Bulgarian Chemical Communications, 42, (2010) 217
[61]. S. Allameh , M.M. Heravi , M.M. Hashemi , F.F. Bamoharram,Chinese Chemical Letters 22 (2011) 131.
[62]. M. Rahimizadeh, T. Bazazan, A. Shiri, M. Bakavoli, H. Hassani Chinese Chemical Letters 22 (2011) 435
[63]. A.Gharib, N. N. Pesyan, M.Jahangir , M. Roshani , J. (H) W.Scheeren Bulgarian Chemical Communications, Volume 44 (2012)11
[64]. A.Gharib , M. Jahangir, M. Roshani, Bulgarian Chemical Communications, 44, (2012)113
[65]. A.Gharib , B. R. H. Khorasani, M. Jahangir , M. Roshani,Bulgarian Chemical Communications, 45(2013) 59
[66]. A.Gharib , B. R. H. Khorasani , M. Jahangir , J. (H) W. Scheeren, Bulgarian Chemical Communications, 45(2013) 64
[67]. G. A. Pasquale, D. M. Ruiz, .J. L. Jios , J.C. Autino , G.P. Romanelli, Tetrahedron Letters 54 (2013) 6574–6579
[68]. C.Jahier a, S. S. Mal, R. A-Oweini , U. Kortz, S.Nlate, Polyhedron 57 (2013) 573
[69]. A. Hafizi, A. Ahmadpour, M. M. Heravi, and F. F. Bamoharram, Petroleum Science and Technology, 32(2014) 1022
[70]. D.Azarifar∗, S-M Khatami and R. N-yami,J. Chem. Sci. 126, (2014) 95
[71]. A.G. Sathicq, D.M. Ruiz, T. Constantieux, J. Rodriguez, G.P. Romanelli, Synlett 25 (2014) 0881
[72]. G. P. Romanelli, E.G. Virla, P.R. Duchowicz, A.L. Gaddi, D. M. Ruiz, d. O. Bennardi,e. D.V. Ortiz,j. C. Autino,J. Agric. Food Chem. 58 (2010) 6290
[73]. E.R-Seresht, R. Tayebee, J. Chem. Pharm. Res., 3(2011) 103
[74]. Y. Zhoua, L. Zheng, F. Hana, G. Zhang, Y.Ma, J. Yao, B. Keita ,P.de Oliveira, L.Nadjo, Colloids and Surfaces A: Physicochem. Eng. Aspects 375 (2011) 97
[75]. C.L. Hill,J. M. S. Weeks,R. F. Schinazi, J. Med. Chem. 33(1990) 2767
[76]. M-H Chiang, M. R. Antonio, C. W. Williams and, L. Soderholm, DaltonTrans. 801(2004)
[77]. C.Bo, J. M. Poblet, Isr. J. Chem. 51(2011) 228
[78]. Xavier L´opez,a Jorge A. Fern´andezb and Josep M. Poblet, Dalton Trans. (2006) 1162
[79]. J.A. Ferna´ndez, X. Lo´pez,, C. Bo,,| C.de Graaf, E.J. Baerends,Josep M. Poblet J. Am. Chem. Soc. 129(2007)12244
[80]. L Yan, X Lo´pez, J. J. Carbo´ , R Sniatynsky,D. C. Duncan,J. M. Poblet J. Am. Chem. Soc. 130(2008) 8223
[81]. S. C-Serra,J. M. C-Juan, E. Coronado,A. G-Ariño, A. Camón, M. Evangelisti, F. Luis, M. J. M-Pérez, J. Sesé, J. Am. Chem. Soc. 134 (2012) 14982
[82]. V. Ball,M. B-Stuckart & Ulrich Kortz, Colloid Polym Sci 291 (2013)1219